The Hippo network kinase STK38 contributes to protein homeostasis by inhibiting BAG3-mediated autophagy

Christina Klimek[a], Judith Wördehoff[a], Ricarda Jahnke[a], Barbara Kathage[a], Daniela Stadel[b], Christian Behrends[c], Alexander Hergovich[d] & Jörg Höhfeld[a]*

[a]Institute for Cell Biology, University of Bonn, Ulrich-Haberland-Str. 61a, 53121 Bonn, Germany;

[b]Institute of Biochemistry II, Goethe University Medical School, Theodor-Stern-Kai 7, 60590 Frankfurt am Main, Germany;

[c]Munich Cluster for Systems Neurology, Ludwig-Maximilians-University Munich, Feodor-Lynen Strasse 17, 81377 München, Germany;

[d]UCL Cancer Institute, University College London, London, WC1E 6BT, UK;

*corresponding author:

Dr. Jörg Höhfeld
Institute for Cell Biology
Rheinische Friedrich-Wilhelms-University Bonn
Ulrich-Haberland-Str. 61a
D-53121 Bonn
Germany
phone: +49 228 735308
fax: +49 228 735302
hoehfeld@uni-bonn.de

Abstract

Chaperone-assisted selective autophagy (CASA) initiated by the cochaperone Bcl2-associated athanogene 3 (BAG3) represents an important mechanism for the disposal of misfolded and damaged proteins in mammalian cells. Under mechanical stress, the cochaperone cooperates with the small heat shock protein HSPB8 and the cytoskeleton-associated protein SYNPO2 to degrade force-unfolded forms of the actin-crosslinking protein filamin. This is essential for muscle maintenance in flies, fish, mice and men. Here, we identify the serine/threonine protein kinase 38 (STK38), which is part of the Hippo signaling network, as a novel interactor of BAG3. STK38 was previously shown to facilitate cytoskeleton assembly and to promote mitophagy as well as starvation and detachment induced autophagy. Significantly, our study reveals that STK38 exerts an inhibitory activity on BAG3-mediated autophagy. Inhibition relies on a disruption of the functional interplay of BAG3 with HSPB8 and SYNPO2 upon direct binding of STK38 to the cochaperone. Of note, STK38 attenuates CASA independently of its kinase activity, whereas previously established regulatory functions of STK38 involve target phosphorylation. The ability to exert different modes of regulation on central protein homeostasis (proteostasis) machineries apparently allows STK38 to coordinate the execution of diverse macroautophagy pathways and to balance cytoskeleton assembly and degradation.

Abbreviations: BAG3, BCL2-associated athanogene; CASA, chaperone-assisted selective autophagy; CHIP, carboxy terminus of HSP70 interacting protein; EPS, electrical pulse stimulation; MBP, maltose-binding protein; mTOR, mammalian target of rapamycin; mTORC1, mammalian target of rapamycin complex 1; STK38, serine/threonine protein kinase 38.

INTRODUCTION

In eukaryotic cells, macroautophagy mediates the degradation of intracellular content by lysosomal hydrolytic enzymes (Lamb *et al.*, 2013; Feng *et al.*, 2014). It involves content enclosure by phagophore membranes, followed by fusion of the formed autophagosome with a lysosome. Autophagy was initially described as a rather unselective pathway induced under starvation conditions, when the digestion of surplus cellular material is essential for survival (Ohsumi, 2014). Since then, an increasing number of selective autophagy pathways has been identified for the regulated degradation of diverse types of cargo, including invading pathogens, dysfunctional organelles and protein aggregates (Yorimitsu and Klionsky, 2005; Feng *et al.*, 2015; Khaminets *et al.*, 2016). Pathways are distinguished by the participating cargo recognition system, often involving specialized ubiquitin conjugation machineries that label the cargo for autophagic degradation, and by the engaged adaptor protein, which links the selected cargo to the phagophore membrane (Khaminets *et al.*, 2016). Moreover, different protein assemblies can initiate autophagosome formation such as the BECN1-RALB-exocyst complex or heteromeric complexes formed by tripartite motif (TRIM) proteins (Antonioli *et al.*, 2017). Evidently, macroautophagic degradation in eukaryotic cells does not rely on a single common machinery but involves a plethora of diverse pathways. Yet, our understanding about the separation, integration and coordination of these pathways is still very limited.

BAG3 initiates the degradation of misfolded, damaged and aggregation-prone proteins through chaperone-assisted selective autophagy (CASA) (Carra *et al.*, 2008; Gamerdinger *et al.*, 2009; Arndt *et al.*, 2010; Behl, 2016; Klimek *et al.*, 2017). In neurons, BAG3-mediated autophagy contributes to the degradation of the Alzheimer-associated protein tau and pathological forms of Huntingtin and SOD1, which are causative agents of Huntington's disease and amyotrophic lateral sclerosis, respectively (Carra *et al.*, 2008; Crippa *et al.*, 2010; Gamerdinger *et al.*, 2011; Lei *et al.*, 2015). In mechanically stressed cells, the pathway mediates the degradation of the actin-crosslinking protein filamin and possibly other mechanosensory proteins (Arndt *et al.*, 2010). Under mechanical stress, filamin undergoes cycles of force-induced unfolding and refolding, which provides the structural flexibility necessary for maintaining actin contacts in this situation (Rognoni *et al.*, 2012; Nakamura *et al.*, 2014). The BAG3 chaperone machinery monitors the conformational state of filamin

and degrades mechanically damaged forms through CASA (Arndt *et al.*, 2005). In agreement with a central role of BAG3 in mechanical stress protection, BAG3 was found to be essential for muscle maintenance in diverse model organisms and BAG3 impairment causes muscle dystrophy and cardiomyopathy in humans (Homma *et al.*, 2006; Selcen *et al.*, 2009; Arndt *et al.*, 2010; Jaffer *et al.*, 2012; Ruparelia *et al.*, 2014; Konersman *et al.*, 2015; Fang *et al.*, 2017; Schänzer *et al.*, 2018).

Client proteins are recognized by BAG3 in conjunction with its chaperone partners, including cytosolic members of the HSP70 chaperone family, i.e. constitutively expressed HSC70/HSPA8, and small heat shock proteins such as HSPB8 (Rauch and Gestwicki, 2014; Rauch *et al.*, 2017). BAG3 then promotes the ubiquitylation of bound clients and their sequestration in perinuclear aggregates as a prerequisite for autophagic degradation (Arndt *et al.*, 2010; Crippa *et al.*, 2010; Gamerdinger *et al.*, 2011; Ulbricht *et al.*, 2013; Guilbert *et al.*, 2018). The generated ubiquitin signal is recognized by the autophagy adaptor SQSTM1/p62, which links the ubiquitylated cargo to phagophore membranes (Gamerdinger *et al.*, 2009). Finally, cargo enclosure can be facilitated through cooperation of BAG3 with SYNPO2 (also known as myopodin) (Ulbricht *et al.*, 2013). The protein recruits a membrane fusion machinery, which mediates autophagosome formation around CASA complexes.

Of note, BAG3 exerts proteostasis functions that go beyond its involvement in autophagy (Klimek *et al.*, 2017). In mechanically stressed cells, the cochaperone stimulates filamin transcription through engagement in the Hippo signaling pathway and increases protein synthesis by regulating the mTOR kinase (Ulbricht *et al.*, 2013; Kathage *et al.*, 2017). Both measures are necessary to counteract the autophagic disposal of damaged filamin and to maintain the actin cytoskeleton under mechanical stress.

The Hippo pathway was first characterized as a linear kinase cascade that controls tissue growth (Yu and Guan, 2013). In mammals, the pathway comprises the serine/threonine protein kinases 3 and 4 (STK3 and STK4, homologs of the *D. melanogaster* kinase Hippo) and the large tumor suppressor kinases 1 and 2 (LATS1 and LATS2). STK3/4 phosphorylate and activate LATS1/2, which in turn phosphorylate the transcriptional coactivators YAP and TAZ, causing their inactivation through cytoplasmic retention. When the pathway is switched off, for example in response to increased mechanical forces, YAP and TAZ migrate into the

nucleus and stimulate the expression of target genes, including filamin (Dupont *et al.*, 2011; Yu and Guan, 2013). The concept of a linear pathway, however, was recently revisited based on the identification of additional kinases that participate in Hippo signaling (Hergovich, 2016). The serine/threonine protein kinase 38 (STK38, also known as nuclear Dbf2-related kinase 1 (NDR1)), for example, was shown to be a substrate of STK3/4 and to phosphorylate YAP (Vichalkovski *et al.*, 2008; Chiba *et al.*, 2009; Tang *et al.*, 2015; Zhang *et al.*, 2015). The data place STK38 at the same stage as LATS1/2 in a Hippo kinase network. Furthermore, STK38 can also be activated by STK24 (Cornils *et al.*, 2011). This extends the network at the initiation level and provides additional means for signal input (Hergovich, 2016). In cardiac muscle cells, STK38-mediated signaling contributes to protein homeostasis through the activation of the RNA binding protein RBM24, which mediates splicing events essential for cardiac development and for the assembly of actin-anchoring structures in this cell type (Poon *et al.*, 2012; Yang *et al.*, 2014; Liu *et al.*, 2017b).

Increasing evidence links the Hippo network to the regulation of autophagy. It was observed that STK3 and STK4 phosphorylate the autophagy membrane marker LC3, which is essential for autophagosome-lysosome fusion (Wilkinson *et al.*, 2015). A prominent role in this functional context is also played by STK38. The kinase stimulates autophagosome formation in response to starvation and cell detachment by positively regulating the BECN1-RALB-exocyst complex (Joffre *et al.*, 2015). Furthermore, STK38 participates in the initiation of mitophagy, a selective autophagy pathway for the degradation of dysfunctional mitochondria (Wu *et al.*, 2013; Bettoun *et al.*, 2016).

Strikingly, our study identifies STK38 as an inhibitor of BAG3-mediated autophagy. Interaction of the kinase with the cochaperone attenuates the autophagic degradation of the BAG3 client filamin and the BAG3 interactor SYNPO2 in adherent smooth muscle cells. Inhibition relies on a remodeling of BAG3 chaperone complexes, which involves a loss of HSPB8 and SYNPO2 binding. Despite the importance of STK38's kinase activity for the regulation of diverse cellular processes such as proliferation or starvation induced autophagy (Cornils *et al.*, 2011; Joffre *et al.*, 2015), we found that STK38 inhibits CASA in a kinase activity independent manner. Our findings illustrate the intensive crosstalk between the BAG3 chaperone machinery and the Hippo signaling network and reveal STK38 as a cellular switch

that coordinates diverse macroautophagy pathways and adjusts assembly and degradation processes during cytoskeleton homeostasis.

RESULTS

STK38 interacts with BAG3

BAG3 initiates the degradation of misfolded, damaged and aggregation-prone proteins through CASA by interacting with diverse partner proteins (Fig. 1A) (Arndt *et al.*, 2010; Crippa *et al.*, 2010; Gamerdinger *et al.*, 2011; Ulbricht *et al.*, 2013; Rauch and Gestwicki, 2014; Kathage *et al.*, 2017; Klimek *et al.*, 2017; Rauch *et al.*, 2017). To further elucidate the BAG3 interactome, an hemagglutinin (HA) tagged form of the cochaperone was expressed in human HEK293T cells followed by BAG3 complex isolation and mass spectrometry, according to previously established procedures (Behrends *et al.*, 2010). Several known BAG3 interactors were detectable in the isolated complexes, including HSC70, HSPB8, CHIP and filamin (isoform FLNA) (Supplemental Table S1). In addition, the kinase STK38 was found associated with the cochaperone. Although STK38 was not among the highest scoring interactors, several features of the protein caught our interest. STK38 is part of the Hippo signaling network, which is regulated by BAG3. Moreover, the kinase is involved in the regulation of cytoskeleton assembly and diverse macroautophagy pathways (Wu *et al.*, 2013; Joffre *et al.*, 2015; Bettoun *et al.*, 2016; Liu *et al.*, 2017a, 2017b). We therefore decided to further investigate the interaction and possible functional interplay of STK38 with BAG3.

As a first step, the observed interaction was verified for endogenous proteins. An anti-BAG3 antibody was used for immunoprecipitation of endogenous BAG3 complexes from A7r5 rat smooth muscle cells, which were subsequently probed for the presence of STK38 (Fig. 1B). The kinase was readily detectable in the isolated BAG3 complexes, pointing to a physiologically relevant interaction.

To investigate whether STK38 interacts directly with BAG3, in-vitro binding studies were performed with purified components. Because we were unable to obtain soluble full-length STK38 through recombinant expression in bacterial cells, deletion fragments of the kinase fused to the maltose-binding protein (MBP) were used in this experiment (Fig. 1C). MBP or MBP-STK38 fusion proteins were immobilized on an amylose resin and incubated with purified BAG3, followed by washing steps to

remove unbound protein. Of note, the cochaperone was retained on an affinity resin that displayed the carboxy-terminal fragment (aa 301-465) of STK38 fused to MBP, whereas retention was not observed on MBP itself (Fig. 1D). A very weak retention of BAG3 was also detected on affinity resins carrying residues 1-150 and 150-300 of STK38. It remains to be seen whether this low affinity binding to the amino-terminal portions of STK38 is of relevance in the cellular environment. In any case, the data reveal a direct interaction between STK38 and BAG3 mainly involving the carboxy-terminus of the Hippo kinase.

STK38 inhibits CASA

To analyze functional consequences of the STK38-BAG3 interaction, the CASA-mediated turnover of the actin-crosslinking protein filamin was investigated. A7r5 rat smooth muscle cells were grown on the extracellular matrix protein fibronectin to induce mechanical tension within the actin cytoskeleton based on cell-matrix contacts. Under these conditions, ~ 40% of the cellular filamin was degraded during inhibition of protein synthesis by cycloheximide for 16 hours (Fig. 2A). This is consistent with previous findings, which showed that degradation is dependent on BAG3 and SYNPO2 and requires inhibition of the mTOR kinase (Ulbricht *et al.*, 2013; Kathage *et al.*, 2017). To verify the impact of STK38 on filamin turnover, the kinase was depleted in A7r5 cells by siRNA transfection (Fig. 2B). Of note, STK38 depletion significantly stimulated filamin degradation, leading to a reduction by about 60% (Fig. 2A). This finding points to an inhibitory role of STK38 in the regulation of BAG3-mediated autophagy.

In addition to filamin, the degradation of SYNPO2 was investigated. Isoforms of SYNPO2, which possess an amino-terminal PDZ domain, i.e. SYNPO2a, b and c (isoforms b and c cannot be distinguished by SDS-PAGE because of similar molecular weight, Fig. 2C), cooperate with BAG3 to initiate autophagy and are co-degraded during the process (see Fig. 1A) (Ulbricht *et al.*, 2013). SYNPO2 turnover can therefore be used as a readout for CASA activity. Cycloheximide shut-off experiments, performed with adherent A7r5 smooth muscle cells, revealed rapid degradation of SYNPO2 (Fig. 2C and D). Notably, degradation was significantly stimulated upon depletion of STK38, similar to findings for filamin turnover. Moreover, treatment with chloroquine (CQ), which inhibits CASA and other autophagic degradation pathways, attenuated SYNPO2 degradation in STK38 depleted cells

(Fig. 2C and D). These data further support an inhibitory activity of STK38 in CASA regulation.

Besides knockdown experiments also overexpression studies were performed. Elevating the cellular concentration of STK38 blocked the degradation of filamin, in agreement with a role of STK38 as a CASA inhibitor (Fig. 2E). In parallel, we also expressed a variant of STK38 that completely lacks any kinase activity due to a lysine to arginine exchange at position 118 (STK38-K118R) (Tamaskovic *et al.*, 2003; Hergovich *et al.*, 2005; Cook *et al.*, 2014). Notably, this kinase-dead variant attenuated SYNPO2 turnover like the wild-type protein (Fig. 2E). Thus, STK38 inhibits CASA in a kinase activity independent manner.

STK38 expression and CASA activity are regulated under mechanical stress

CASA is induced in mechanically stressed cells and tissues, when cytoskeleton components become unfolded and are damaged by mechanical force (Ulbricht *et al.*, 2013, 2015). Cytoskeleton contraction and damage were triggered in differentiated murine C2C12 myotubes through electrical pulse stimulation (EPS) according to previously established protocols (Orfanos *et al.*, 2016). Subsequently, mechanical stress dependent changes in protein abundance were monitored. EPS caused an immediate increase in BAG3 expression and a rapid decline of filamin levels in mechanically stressed myotubes during the first hour of treatment, reflecting force-induced CASA activity (Fig. 2F and G). At subsequent time points, however, filamin levels remained constant despite elevated BAG3 expression. Strikingly, the attenuation of filamin degradation coincided with an upregulation of STK38 expression at late time points (Fig. 2F and G). STK38 upregulation may thus limit CASA activity upon severe and prolonged mechanical stress, when over-excessive degradation of cytoskeleton components would contribute to a collapse of the cellular architecture, and may initiate repair processes based on an STK38-dependent stimulation of cytoskeleton assembly (Liu *et al.*, 2017a).

The STK38 upstream kinases STK3, STK4 and STK24 participate in CASA regulation

STK38 is part of the Hippo signaling network (Yu and Guan, 2013). STK3 and STK4 act upstream of STK38 and are able to activate the kinase (Vichalkovski *et al.*, 2008; Chiba *et al.*, 2009; Tang *et al.*, 2015). Furthermore, the kinase STK24 can positively

regulate STK38 through phosphorylation (Cornils *et al.*, 2011). We investigated whether STK3, STK4 and STK24 participate in the regulation of CASA. Expression of the kinases was reduced by transient transfection of A7r5 cells with corresponding siRNAs, as verified through transcript quantification (Fig. 3A). To monitor consequences for SYNPO2 degradation, cycloheximide shut-off experiments were performed (Fig. 3B and C). Depletion of STK3 or STK4 attenuated the degradation of SYNPO2 during cycloheximide treatment, indicating that these kinases are required for the execution of CASA (Fig. 3B). Notably, STK3 and STK4 were previously identified as essential autophagy regulators, which mediate the phosphorylation of the autophagosome membrane marker LC3 to facilitate autophagosome-lysosome fusion (Wilkinson *et al.*, 2015). The observed inhibition of SYNPO2 degradation may thus reflect a general requirement of STK3 and STK4 for macroautophagic degradation.

In contrast to findings for STK3 and STK4, depletion of STK24 stimulated the turnover of SYNPO2 in adherent A7r5 cells (Fig. 3B). Moreover, also filamin degradation was increased upon STK24 depletion (Fig. 3C). Thus, the data for STK24 mirror those obtained for STK38 (see above). Our findings suggest that STK24 cooperates with STK38 on a signaling pathway that limits CASA activity in mammalian cells.

STK24 phosphorylates STK38 on threonine 444 (T444) (Cornils *et al.*, 2011). A mutant form of STK38, which cannot be phosphorylated due to a threonine to alanine exchange at this position (T444A), was used to explore the importance of STK38 regulation for CASA inhibition. In contrast to wild-type STK38, the mutant form did not significantly attenuate filamin degradation upon overexpression in adherent A7r5 smooth muscle cells (Fig. 3D). Because T444 phosphorylation could affect binding of STK38 to BAG3, association between both proteins was analyzed. HeLa cells were transiently transfected with plasmid constructs encoding epitope-tagged forms of BAG3 and STK38, STK38-K118R or STK38-T444A, followed by BAG3 complex isolation and detection of STK38 variants in these complexes (Fig. 3E). Similar levels of wild-type STK38 and the kinase-dead variant K118R were found associated with immunoprecipitated BAG3 (Fig. 3E and F). However, the T444A variant, although expressed at the same level as STK38 and STK38-K118R, was recovered to a lesser extent in BAG3 complexes compared to the other variants (Fig. 3E and F). Taken together, our data suggest that phosphorylation of STK38 at

threonine 444 by upstream kinases such as STK24 promotes the association of STK38 with BAG3 for efficient inhibition of CASA activity.

CASA is initiated independently of the STK38 targets BECN1 and RALB

During starvation and detachment induced autophagy, STK38 interacts with the autophagy regulator BECN1 to promote its association with RALB and the exocyst membrane tethering complex at initial stages of autophagosome formation (Joffre *et al.*, 2015). This stimulating function, which is dependent on the kinase activity of STK38 (Joffre *et al.*, 2015; Bettoun *et al.*, 2016), is in sharp contrast to the inhibitory and kinase activity independent function exerted by STK38 in the context of CASA (see Fig. 2). Autophagosome membrane formation and expansion during CASA may thus mechanistically differ from early stages of the other autophagy pathways. To verify this, BECN1 and RALB were depleted from A7r5 smooth muscle cells (Fig. 4A), and consequences for CASA activity were investigated by monitoring the turnover of SYNPO2 and filamin in cycloheximide shut-off experiments. Notably, BECN1 and RALB depletion, respectively, did not have any significant effect on the degradation of SYNPO2 or filamin (Fig. 4B and C). CASA apparently proceeds in a BECN1 and RALB independent manner, providing a molecular basis for the different mode of regulation exerted by STK38 on CASA in comparison to other macroautophagy pathways.

STK38 disrupts the interaction of BAG3 with HSPB8 and SYNPO2

Next, we sought to elucidate the molecular basis for the inhibitory function of STK38 in CASA regulation. In particular, the impact of STK38 on the composition of BAG3 chaperone complexes was investigated. For this purpose, STK38 and BAG3 were transiently overexpressed in HeLa cells, followed by immunoprecipitation of BAG3 complexes (Fig. 5A). Purified matrix-bound complexes were incubated with ATP, which disrupts the interaction of BAG3 with the ATP-regulated chaperone HSC70 and causes partial release of non-antibody bound BAG3 from oligomeric chaperone complexes (Fig. 5A). Binding of BAG3 to the small heat shock protein HSPB8 is not ATP-sensitive (Arndt *et al.*, 2010; Rauch *et al.*, 2017). Indeed, HSPB8 was only detectable in eluates obtained after glycin-induced disruption of the antibody-antigen interaction (Fig. 5A). Most notably, the presence of STK38 in BAG3 complexes had a

profound impact on the protein composition of these complexes. It strongly reduced the binding of HSPB8 to BAG3 (Fig. 5A).

STK38 exerts its CASA inhibiting activity in a kinase independent manner (see Fig. 2E). Therefore, we also investigated whether the kinase-dead variant of STK38 (STK38-K118R) affects BAG3 complex composition. As is evident from figure 5A, association of STK38-K118R with BAG3 disrupted the interaction of the cochaperone with HSPB8. The kinase-dead variant thus behaves like the wild-type protein, further demonstrating the kinase activity independent mode of regulation that is exerted by STK38 on BAG3.

We had previously observed that SYNPO2 could not be detected in BAG3 complexes isolated by immunoprecipitation (Ulbricht *et al.*, 2013). To verify, whether STK38 also affects the interaction between BAG3 and SYNPO2, we isolated SYNPO2 complexes and monitored the presence of the cochaperone in these complexes. For this purpose, SYNPO2 was transiently overexpressed in HeLa cells alone or together with STK38 or the kinase-dead variant, and an anti-SYNPO2 antibody was subsequently used for complex isolation by immunoprecipitation. While BAG3 was associated with SYNPO2 under control conditions, the cochaperone was not detectable in SYNPO2 complexes upon overexpression of STK38 or STK38-K118R (Fig. 5B). Moreover, neither variant of STK38 could be detected in association with SYNPO2. Binding of STK38 or STK38-K118R to BAG3 apparently disrupts the interaction of the cochaperone with SYNPO2. Taken together, our experiments reveal a kinase-independent ability of STK38 to remodel BAG3 chaperone complexes, leading to a loss of HSPB8 and SYNPO2 (Fig. 5C). Because both proteins cooperate with BAG3 during CASA (see Fig. 1A) (Carra *et al.*, 2008; Arndt *et al.*, 2010; Ulbricht *et al.*, 2013; Guilbert *et al.*, 2018), STK38 binding to BAG3 potently interferes with the execution of the degradation pathway.

DISCUSSION

The Hippo network kinase STK38 is essential for cytoskeleton assembly and for the execution of mitophagy as well as starvation and detachment induced autophagy (Wu *et al.*, 2013; Joffre *et al.*, 2015; Bettoun *et al.*, 2016). Here, we demonstrate that binding of STK38 to the cochaperone BAG3 inhibits the degradation of cytoskeleton proteins through chaperone-assisted selective autophagy. Taken together, it

becomes apparent that STK38 coordinates the execution of diverse macroautophagy pathways and controls cytoskeleton maintenance in mammalian cells (Fig. 5C).

During starvation and detachment induced autophagy, STK38 promotes the formation of the BECN1-RALB-exocyst complex (Joffre *et al.*, 2015). The complex activates the phosphatidylinositol-3 kinase VPS34, which generates PI3P-positive precursor membranes for the recruitment of additional autophagy factors at initial stages of autophagosome formation (Bodemann *et al.*, 2011; Lamb *et al.*, 2013). STK38 also stimulates mitophagy, the autophagic clearance of damaged and depolarized mitochondria (Wu *et al.*, 2013; Bettoun *et al.*, 2016). Mitophagy is triggered by the exposure of ubiquitin chains on the mitochondrial outer membrane, generated by the ubiquitin ligase Parkin (Winklhofer, 2014). Targeting of Parkin to depolarized mitochondria is facilitated by STK38 (Wu *et al.*, 2013). Furthermore, the ability of STK38 to stimulate the formation of the BECN1-RALB-exocyst complex may contribute to the induction of mitophagy, as RALB depletion attenuates STK38-dependent mitophagy in transformed human cells (Bettoun *et al.*, 2016). Importantly, we demonstrate here that CASA proceeds independently of BECN1 and RALB (Fig. 4). This is consistent with a previous study showing that BECN1 is not required for CASA (Merabova *et al.*, 2015). The fact that components, which confer the stimulating activity of STK38 during mitophagy and starvation and detachment induced autophagy, are dispensable for CASA, apparently provides the basis for a different mode of regulation, enabling STK38 to inhibit CASA (Fig. 5C).

Surprisingly, CASA inhibition did not require the kinase activity of STK38. The kinase-dead variant STK38-K118R (Tamaskovic *et al.*, 2003; Hergovich *et al.*, 2005; Cook *et al.*, 2014) attenuated filamin turnover like the wild-type protein upon overexpression in adherent smooth muscle cells (Figs. 2C). Moreover, binding of both forms to BAG3 interfered with the interaction of the cochaperone with HSPB8 and SYNPO2 (Fig. 5A and B). Thus, steric hindrances rather than phosphorylation-induced conformational changes seem to cause the STK38-induced disruption of BAG3 complexes and CASA inhibition. Although independent of the kinase activity of STK38, CASA inhibition nevertheless appears to be a regulated event. The STK38 upstream kinase STK24 (Cornils *et al.*, 2011) also attenuated CASA (Fig. 4), and a mutant form of STK38 that cannot be activated by STK24 (STK38-T444A) displayed reduced BAG3 binding and CASA inhibiting activity (Fig. 4). STK24 and STK38 thus

seem to cooperate on a signaling pathway, which limits autophagic flux through CASA in mammalian cells.

Mechanical force is a major physiological signal in the regulation of the Hippo network and CASA activity (Wackerhage *et al.*, 2014; Klimek *et al.*, 2017). Intriguingly, regulation is inversely correlated. Force generated in adherent cells or contracting muscles stimulates CASA (Ulbricht *et al.*, 2013, 2015), whereas the loss of mechanical cues for example upon cell detachment from the extracellular matrix activates Hippo kinases (Dupont *et al.*, 2011; Wrighton, 2011). In this regard, the observed STK38-mediated regulation of BAG3 seems to represent an important nodal point for co-regulation. Through STK38 and the STK38 upstream kinase STK24, a detachment-induced activation of Hippo kinases would be transferred onto the CASA machinery to switch off the degradation pathway, no longer needed for the disposal of force-unfolded cytoskeleton proteins in this situation. At the same time, core macroautophagy factors would become available for detachment-induced autophagy and mitophagy, which are positively regulated by STK38 (Fig. 5C) (Bettoun *et al.*, 2016; Sharif and Hergovich, 2018). The autophagic degradation of mechanotransducers and adhesion complexes prevents cell death, when cells are deprived of extra cellular matrix contacts, and mitophagy would limit the production of reactive oxygen species in this situation (Fung *et al.*, 2008; Bettoun *et al.*, 2016; Kenific *et al.*, 2016a, 2016b). In a similar manner, STK38-mediated regulation could operate upon nutrient depletion and redirect common macroautophagy factors towards starvation-induced autophagy to ensure survival at the expense of CASA and cytoskeleton quality control.

Importantly, functional cooperation between the Hippo network and the BAG3 chaperone machinery is not a one-way route, on which Hippo signaling controls CASA activity. We previously showed that BAG3 directly interacts with the Hippo kinases LATS1 and LATS2 in a manner that disrupts inhibition of the transcriptional coactivators YAP and TAZ (Ulbricht *et al.*, 2013). The study revealed a BAG3-dependent mechanotransduction pathway that controls downstream components of the Hippo network. On this pathway, accumulation of force-unfolded proteins triggers the activation of the heat shock transcription factor 1 (HSF1), which stimulates BAG3 expression and ultimately YAP/TAZ activation (Ulbricht *et al.*, 2013). Thus, bi-directional crosstalk connects the Hippo network and the BAG3 chaperone machinery.

In striated skeletal and heart muscle, BAG3 is localized at actin-anchoring Z-disks, which limit the contractile sarcomeric unit (Henderson *et al.*, 2017). Loss or functional impairment of the cochaperone in animal models and patients results in a force-induced disintegration of Z-disks and aggregation of Z-disk proteins, leading to severe muscle weakness (Homma *et al.*, 2006; Selcen *et al.*, 2009; Arndt *et al.*, 2010; Ruparelia *et al.*, 2014; Konersman *et al.*, 2015; Ganassi *et al.*, 2016; McClung *et al.*, 2017). Intriguingly, knockdown of STK38 in cardiac muscle cells essentially mirrors the phenotype caused by BAG3 depletion or impairment. It also triggers Z-disk disintegration and aggregate formation (Liu *et al.*, 2017b). Muscle specific functions of STK38 were initially attributed to the regulation of the RNA-binding protein RBM24 (Liu *et al.*, 2017a). However, based on the findings reported here, we would propose that dysregulated disposal of Z-disk components significantly contributes to the collapse of the sarcomeric architecture observed upon loss of STK38. Indeed, similar to the accelerated turnover of filamin and SYNPO2 demonstrated by us in STK38-depleted smooth muscle cells (see Fig. 2), knockdown of the kinase in cardiac muscle cells stimulated the degradation of several Z-disk and cytoskeleton proteins (Liu *et al.*, 2017b). Apparently, STK38 fulfills a central role in the balancing of anabolic and catabolic processes in muscle cells.

EXPERIMENTAL PROCEDURES

Antibodies

The following antibodies were used for protein detection: anti-BAG3 (rabbit; 10599-1-AP, Proteintech Group), anti-BECN1 (rabbit, #8676, Cell Signaling), anti-γ-tubulin (mouse; T5326, Sigma Aldrich), anti-filamin (rabbit; generously provided by D. Fürst, Bonn), anti-HA (rabbit, sc-805, Santa Cruz), anti-HSC70 (rabbit, generated against purified HSC70 (Höhfeld and Jentsch, 1997)), anti-HSPB8 (rabbit, STJ24102, St John´s Lab), anti-MBP (mouse, ab23903, Abcam), anti-RALB (rabbit, STJ28797, St John´s Lab), anti-STK38 (mouse, ABIN564919, Abnova), anti-SYNPO2 (rabbit; generated by Dieter Fürst, Bonn) and rabbit IgG (sc-2027, Santa Cruz).

BAG3 interactome proteomic analysis

HEK293T human embryonic kidney cells (Sigma Aldrich, #12022001) stably expressing N-terminally HA-tagged BAG3 were harvested and lysed with 3 ml lysis buffer (50 mM Tris, pH 7.5, 150 mM NaCl, 0.5% Nonidet P40 (NP40) and EDTA-free protease inhibitor cocktail tablets). Centrifugation-cleared lysates (16,000 x g) were filtered through 0.45 µm spin filters (Millipore Ultrafree-CL) and immunoprecipitated with 60 µl anti-HA resin. Resin containing immune complexes were washed five times with lysis buffer followed by five PBS washes, and elution with 150 µl of 250 mg/ml HA peptide in PBS. Eluted immune complexes were precipitated with 20% trichloroacetic acid (TCA) and pellets were washed once with 10% TCA and four times with cold acetone. Precipitated proteins were resuspended in 50 mM ammonium bicarbonate (pH 8.0) with 20% acetonitrile and incubated with sequencing grade trypsin at a concentration of 12.5 ng/ml at 37ºC for 4 h. Trypsin reactions were quenched by addition of 5% formic acid and peptides were desalted using C18 Stage Tips. For each liquid chromatography coupled to tandem mass spectrometry run using an LTQ Velos linear ion trap mass spectrometer (Thermo Scientific), 4 µl were loaded onto a 18 cm x 125 µm (ID) C18 column and peptides eluted using a 50 min 8–26% acetonitrile gradient. Spectra were acquired using a data-dependent Top-10 method. Each sample was shot twice in succession, followed by a wash with 70% acetonitrile and 30% isopropanol. Tandem MS/MS data were searched using Sequest and a concatenated target-decoy uniprot human database with a 2 Da mass

window. All data were filtered to a 1% false discovery rate (peptide level) before analysis using CompPASS (Sowa *et al.*, 2009).

Protein expression and purification

STK38 encoding cDNA fragments (corresponding to aa 1-150, aa 150-300, aa 301-465 of STK38) were subcloned into pMal vector (New England Biolabs). Resultant constructs were used for expression of MBP fusion proteins in *E. coli* TG1 cells, followed by purification on an amylose resin according to the manufacturer's protocol (New England Biolabs). Prior to final elution, isolated complexes were incubated with 2 mM ATP, 1 mM $MgCl_2$, 20 mM MOPS pH 7.2, 100 mM KCl to dissociate bacterial HSP70. BAG3 encoding cDNA, subcloned into pET-M11 (Novagene), was used for expression of HIS-fusion proteins in *E. coli* BL21(DE3) and purified on Ni-NTA-agarose as described by the manufacturer (Qiagen). Before elution an additional washing step with MgATP was performed.

In-vitro binding studies

To verify binding of BAG3 to STK38 fragments, MBP-STK38 and MBP fragments (2 µM) were incubated with amylose beads in binding buffer (20 mM MOPS-KOH, pH 7.5, 100 mM KCl, 0.5% Tween 20) for 1 h at 4°C, followed by addition of His-BAG3 (0.4 µM) for 1 h at 4°C. Beads were collected by centrifugation at 800 x g for 3 min and washed four times with washing buffer (20 mM MOPS-KOH, pH 7.5, 100 mM KCl, 0.5% Tween 20) and two times with washing buffer without Tween 20. Retained proteins were finally eluted with elution buffer (20 mM MOPS-KOH, pH 7.2, 100 mM KCl, 20 mM maltose). Eluted proteins were precipitated in 10% trichloroacetic acid and analyzed by immunoblotting.

siRNAs and cell techniques

FlexiTube siRNAs (Qiagen) were handled according to the manufacturer. Allstars negative control siRNA (Qiagen) was used as a control. A7r5 rat smooth muscle embryonic aorta cells (Sigma Aldrich, #86050803) were cultured in Dulbecco's Modified Eagle Medium (DMEM) containing 10% fetal calf serum, L-glutamine and penicillin/streptomycin (PS), at 37°C and 5% CO_2. When indicated, cells were transfected with JetPRIME transfection reagent (Peqlab) following manufacturer's instructions with either plasmid DNA or siRNA. For transient transfection HeLa cells

were grown to 40% confluency in a 10 cm dish. Cells were transfected with a calcium phosphate transfection method using 1.4 ml transfection solution (155 mM $CaCl_2$, 137 mM NaCl, 5 mM KCl, 0.7 mM Na_2HPO_4, 7.5 mM glucose, 21 mM HEPES) containing 6-18 µg DNA. The transfection solution was replaced with culture medium after 16 h. Two days after transfection, cells were lysed in RIPA buffer (25 mM Tris-HCl, pH 8.0, 150 mM NaCl, 0.5% sodium deoxycholate, 1% Nonidet P-40, 0.1% SDS, 10% glycerol, complete protease inhibitor (Roche), phosSTOP phosphatase inhibitor (Roche)) and incubated on ice for 20 min. Lysates were centrifuged at 16,000 x g for 20 min at 4°C. Supernatants were collected and analyzed by immunoblotting.

To monitor SYNPO2 degradation, protein synthesis was inhibited in A7r5 cells by treatment with 50 µM cycloheximide (Roth) for indicated times prior to cell lysis. Cells were lysed as described above and protein degradation was analyzed by immunoblotting. SYNPO2 levels were quantified by densitometry and normalized to γ-tubulin levels. Level at time point zero was set to 1.

To analyze filamin degradation, A7r5 cells were seeded 48 h post transfection on fibronectin (1.25 µg/cm^2, BD Biosciences) coated culture dishes for 24 h. Prior to cell lysis, cells were treated with 50 µM cycloheximide (Roth) for 16 h to inhibit protein synthesis (corresponding to time point zero of the experiment). Protein degradation was analyzed by immunoblotting. Filamin levels were quantified and normalized to γ-tubulin levels.

Immunoprecipitation

To isolate protein complexes by immunoprecipitation with an anti-FLAG (M2) antibody, HeLa cells (Sigma Aldrich, #93021013) were transfected with plasmids encoding FLAG-BAG3, FLAG-SYNPO2a, FLAG-STK38 (wild-type) and FLAG-STK38-K118R (kinase-dead variant), respectively. When indicated cells were also transfected with plasmids encoding HA-STK38, HA-STK38-K118R and HA-STK38-T444A (Cook *et al.*, 2014). Two days after transfection, cells were sonicated in lysis buffer (25 mM Tris-HCl, pH 8,0, 150 mM NaCl, 0.5% sodium deoxycholate, 1% Nonidet P-40, 10% glycerol, 2 mM EDTA, complete protease inhibitor (Roche)) for 20 min followed by centrifugation at 16,000 x g for 20 min at 4°C. The supernatant was adjusted to a protein concentration of 10 mg/ml. Samples were incubated with anti-FLAG M2 agarose (Sigma) (30 µl resin per 1 ml extract) for 1 h at 4°C on a

rotation wheel. Agarose beads were collected by centrifugation at 800 x g for 5 min at 4°C, followed by washing four times with RIPA buffer und two times with wash buffer (20 mM MOPS pH 7.2, 100 mM KCl). When indicated, beads were incubated in ATP buffer (20 mM MOPS pH 7.2, 100 mM KCl, 2 mM $MgCl_2$, 2 mM ATP) for 30 min at 37°C, prior to final elution with glycine/HCl, pH 3.5. Samples were analyzed by immunoblotting.

When complexes were immunoprecipitated with antibodies directed against SYNPO2 or BAG3, protein G-sepharose (GE Healthcare) (30 µl resin per 1 ml extract) was used together with 12.5 µg of control IgG (rabbit IgG) and the same amount of the anti-SYNPO2 or anti-BAG3 antibody.

Quantitative real time PCR

InviTrap Spin Universal RNA Mini Kit (Stratec) was used to isolate RNA from A7r5 rat smooth muscle cells. cDNA was synthesized from 1 µg RNA by using the iScript cDNA synthesis kit (Bio-Rad). Quantitative PCR (qPCR) was performed using SsoFast™ EvaGreen® Supermix (Bio-Rad). Transcript levels for GAPDH and beta-2-microglobulin (B2M) were monitored as reference transcripts. Relative gene expression was calculated using the ΔΔCT method. The specificity of the PCR amplification was verified by melting curve analysis of the final products using Bio-Rad CFX 3.1 software. For each experiment three biological and three technical replicates were analyzed. The following oligonucleotide primer were used:

STK3 (*Rattus norvegicus*) forward	TACGTCTATAGAAATGGCAGAAGG
STK3 (*Rattus norvegicus*) revers	GATGAAAGGATGCTGTAACAGC
STK4 (*Rattus norvegicus*) forward	GATCAACACGGAGGATGAGG
STK4 (*Rattus norvegicus*) revers	AGCTCTTCAGAAACTCGTAGTC
STK24 (*Rattus norvegicus*) forward	GACAATCGGACTCAGAAAGTGG
STK24 (*Rattus norvegicus*) revers	TTCTAACAGATCCAGGGCAGAG
B2M (*Rattus norvegicus*) forward	GTGATCTTTCTGGTGCTTGTC
B2M (*Rattus norvegicus*) revers	AAGTTGGGCTTCCCATTCTC
GAPDH (*Rattus norvegicus*) forward	GAGAAACCTGCCAAGTATGATGAC
GAPDH (*Rattus norvegicus*) revers	ATCGAAGGTGGAAGAGTGGG

Electrical pulse stimulation

Differentiated C2C12 myotubes grown on 6-well plates were stimulated using a C-dish and the C-Pace unit (Ion Optix, Milton) for 10 msec pulses at 10 V. A pulse program of 5 sec at 15 Hz (tetanic hold), 5 sec pause, 5 sec at 5 Hz (twitch contractions) and 5 sec pause was repeated, for indicated durations, as described previously (Orfanos *et al.*, 2016). Myotubes were harvested in PBS and lysed as described above. Protein level was analyzed by immunoblotting.

Statistics

Quantification of blot lane intensities was accomplished using ImageJ. Data were analyzed for statistical significance using the two-tailed student's t-test. P-value levels derived from student's t-test are shown with significance stars: *p ≤ 0.05, **p ≤ 0.01, ***p ≤ 0.001.

ACKNOWLEDGMENTS

We thank Karen Himmelberg for expert technical assistance and Dieter Fürst for providing antibodies against cytoskeletal proteins. Work was supported by the following grants: DFG EXC 1010 SyNergy and support by the Boehringer Ingelheim Foundation to C.B., Wellcome Trust Research Career Development fellowship 090090/Z/09/Z to A.H., and DFG FOR 1352 TP10, DFG FOR 2743 TP1 and DFG HO 1518/9-1 to J.H.

AUTHOR CONTRIBUTIONS

C.K., J.W., R.J., B.K. and D.S. conducted the experiments.
C.B. supervised the proteomics part of the study.
C.B., A.H. and J.H. designed the experiments, supervised the involved coworkers and discussed the obtained data.
J.H. wrote the manuscript.
C.K., C.B. and A.H. edited the manuscript.

DECLARATION OF INTERESTS

The authors declare no competing interests.

REFERENCES

Antonioli, M., Di Rienzo, M., Piacentini, M., and Fimia, G. M. (2017). Emerging Mechanisms in Initiating and Terminating Autophagy. Trends Biochem. Sci. *42*, 28–41.

Arndt, V. *et al.* (2010). Chaperone-Assisted Selective Autophagy Is Essential for Muscle Maintenance. Curr. Biol. *20*, 143–148.

Arndt, V., Daniel, C., Nastainczyk, W., Alberti, S., and Höhfeld, J. (2005). BAG-2 acts as an inhibitor of the chaperone-associated ubiquitin ligase CHIP. Mol. Biol. Cell *16*, 5891–5900.

Behl, C. (2016). Breaking BAG: The Co-Chaperone BAG3 in Health and Disease. Trends Pharmacol. Sci. *37*, 672–688.

Behrends, C., Sowa, M. E., Gygi, S. P., and Harper, J. W. (2010). Network organization of the human autophagy system. Nature *466*, 68–76.

Bettoun, A. *et al.* (2016). Mitochondrial clearance by the STK38 kinase supports oncogenic Ras-induced cell transformation. Oncotarget *7*, 44142–44160.

Bodemann, B. O. *et al.* (2011). RalB and the Exocyst Mediate the Cellular Starvation Response by Direct Activation of Autophagosome Assembly. Cell *144*, 253–267.

Carra, S., Seguin, S. J., Lambert, H., and Landry, J. (2008). HspB8 chaperone activity toward poly(Q)-containing proteins depends on its association with Bag3, a stimulator of macroautophagy. J. Biol. Chem. *283*, 1437–1444.

Chiba, S., Ikeda, M., Katsunuma, K., Ohashi, K., and Mizuno, K. (2009). MST2- and Furry-mediated activation of NDR1 kinase is critical for precise alignment of mitotic chromosomes. Curr. Biol. *19*, 675–681.

Cook, D., Hoa, L. Y., Gomez, V., Gomez, M., and Hergovich, A. (2014). Constitutively active NDR1-PIF kinase functions independent of MST1 and hMOB1 signalling. Cell. Signal. *26*, 1657–1667.

Cornils, H., Kohler, R. S., Hergovich, A., and Hemmings, B. A. (2011). Human NDR Kinases Control G1/S Cell Cycle Transition by Directly Regulating p21 Stability. Mol. Cell. Biol. *31*, 1382–1395.

Crippa, V. *et al.* (2010). The small heat shock protein B8 (HspB8) promotes autophagic removal of misfolded proteins involved in amyotrophic lateral sclerosis (ALS). Hum. Mol. Genet. *19*, 3440–3456.

Dupont, S. *et al.* (2011). Role of YAP/TAZ in mechanotransduction. Nature *474*, 179–183.

Fang, X. *et al.* (2017). Loss-of-function mutations in co-chaperone BAG3 destabilize small HSPs and cause cardiomyopathy. J. Clin. Invest. *127*, 3189–3200.

Feng, Y., He, D., Yao, Z., and Klionsky, D. J. (2014). The machinery of macroautophagy. Cell Res. *24*, 24–41.

Feng, Y., Yao, Z., and Klionsky, D. J. (2015). How to control self-digestion: transcriptional, post-transcriptional, and post-translational regulation of

autophagy. Trends Cell Biol. *25*, 354–363.

Fung, C., Lock, R., Gao, S., Salas, E., and Debnath, J. (2008). Induction of Autophagy during Extracellular Matrix Detachment Promotes Cell Survival. Mol. Biol. Cell *19*, 797–806.

Gamerdinger, M., Hajieva, P., Kaya, A. M., Wolfrum, U., Hartl, F. U., and Behl, C. (2009). Protein quality control during aging involves recruitment of the macroautophagy pathway by BAG3. EMBO J. *28*, 889–901.

Gamerdinger, M., Kaya, A. M., Wolfrum, U., Clement, A. M., and Behl, C. (2011). BAG3 mediates chaperone-based aggresome-targeting and selective autophagy of misfolded proteins. EMBO Rep. *12*, 149–156.

Ganassi, M. *et al.* (2016). A Surveillance Function of the HSPB8-BAG3-HSP70 Chaperone Complex Ensures Stress Granule Integrity and Dynamism. Mol. Cell *63*, 796–810.

Guilbert, S. M., Lambert, H., Rodrigue, M.-A., Fuchs, M., Landry, J., and Lavoie, J. N. (2018). HSPB8 and BAG3 cooperate to promote spatial sequestration of ubiquitinated proteins and coordinate the cellular adaptive response to proteasome insufficiency. FASEB J. *32*, 3518–3535.

Henderson, C. A., Gomez, C. G., Novak, S. M., Mi-Mi, L., and Gregorio, C. C. (2017). Overview of the Muscle Cytoskeleton. In: Comprehensive Physiology, Hoboken, NJ, USA: John Wiley & Sons, Inc., 891–944.

Hergovich, A. (2016). The Roles of NDR Protein Kinases in Hippo Signalling. Genes (Basel). *7*, 21.

Hergovich, A., Bichsel, S. J., and Hemmings, B. A. (2005). Human NDR Kinases Are Rapidly Activated by MOB Proteins through Recruitment to the Plasma Membrane and Phosphorylation. Mol. Cell. Biol. *25*, 8259–8272.

Höhfeld, J., and Jentsch, S. (1997). GrpE-like regulation of the Hsc70 chaperone by the anti-apoptotic protein BAG-1. EMBO J. *16*, 6209–6216.

Homma, S., Iwasaki, M., Shelton, G. D., Engvall, E., Reed, J. C., and Takayama, S. (2006). BAG3 deficiency results in fulminant myopathy and early lethality. Am. J. Pathol. *169*, 761–773.

Jaffer, F. *et al.* (2012). BAG3 mutations: Another cause of giant axonal neuropathy. J. Peripher. Nerv. Syst. *17*, 210–216.

Joffre, C. *et al.* (2015). The Pro-apoptotic STK38 Kinase Is a New Beclin1 Partner Positively Regulating Autophagy. Curr. Biol. *25*, 2479–2492.

Kathage, B. *et al.* (2017). The cochaperone BAG3 coordinates protein synthesis and autophagy under mechanical strain through spatial regulation of mTORC1. Biochim. Biophys. Acta - Mol. Cell Res. *1864*, 62–75.

Kenific, C. M., Stehbens, S. J., Goldsmith, J., Leidal, A. M., Faure, N., Ye, J., Wittmann, T., and Debnath, J. (2016a). NBR1 enables autophagy-dependent focal adhesion turnover. J. Cell Biol. *212*, 577–590.

Kenific, C. M., Wittmann, T., and Debnath, J. (2016b). Autophagy in adhesion and migration. J. Cell Sci. *129*, 3685–3693.

Khaminets, A., Behl, C., and Dikic, I. (2016). Ubiquitin-Dependent And Independent Signals In Selective Autophagy. Trends Cell Biol. *26*, 6–16.

Klimek, C., Kathage, B., Wördehoff, J., and Höhfeld, J. (2017). BAG3-mediated proteostasis at a glance. J. Cell Sci. *130*, 2781–2788.

Konersman, C. G., Bordini, B. J., Scharer, G., Lawlor, M. W., Zangwill, S., Southern, J. F., Amos, L., Geddes, G. C., Kliegman, R., and Collins, M. P. (2015). BAG3 myofibrillar myopathy presenting with cardiomyopathy. Neuromuscul. Disord. *25*, 418–422.

Lamb, C. A., Yoshimori, T., and Tooze, S. A. (2013). The autophagosome: origins

unknown, biogenesis complex. Nat. Rev. Mol. Cell Biol. *14*, 759–774.
Lei, Z., Brizzee, C., and Johnson, G. V. W. (2015). BAG3 facilitates the clearance of endogenous tau in primary neurons. Neurobiol. Aging *36*, 241–248.
Liu, J., Kong, X., Lee, Y. M., Zhang, M. K., Guo, L. Y., Lin, Y., Lim, T. K., Lin, Q., and Xu, X. Q. (2017a). Stk38 Modulates Rbm24 Protein Stability to Regulate Sarcomere Assembly in Cardiomyocytes. Sci. Rep. *7*, 44870.
Liu, J., Kong, X., Yew Mun, L., Meng Kai, Z., Li Yan, G., Lin, Y., Lim, T. K., Lin, Q., and Xu, X. Q. (2017b). Stk38 Modulates Rbm24 Protein Stability to Regulate Sarcomere Assembly in Cardiomyocytes. Sci. Rep. *7*, 44870.
McClung, J. M. *et al.* (2017). BAG3 (Bcl-2–Associated Athanogene-3) Coding Variant in Mice Determines Susceptibility to Ischemic Limb Muscle Myopathy by Directing AutophagyClinical Perspective. Circulation *136*, 281–296.
Merabova, N., Sariyer, I. K., Saribas, A. S., Knezevic, T., Gordon, J., Turco, M. C., Rosati, A., Weaver, M., Landry, J., and Khalili, K. (2015). WW Domain of BAG3 Is Required for the Induction of Autophagy in Glioma Cells. J. Cell. Physiol. *230*, 831–841.
Nakamura, F., Song, M., Hartwig, J. H., and Stossel, T. P. (2014). Documentation and localization of force-mediated filamin A domain perturbations in moving cells. Nat. Commun. *5*, 4656.
Ohsumi, Y. (2014). Historical landmarks of autophagy research. Cell Res. *24*, 9–23.
Orfanos, Z., Gödderz, M. P. O., Soroka, E., Gödderz, T., Rumyantseva, A., van der Ven, P. F. M., Hawke, T. J., and Fürst, D. O. (2016). Breaking sarcomeres by in vitro exercise. Sci. Rep. *6*, 19614.
Poon, K. L., Tan, K. T., Wei, Y. Y., Ng, C. P., Colman, A., Korzh, V., and Xu, X. Q. (2012). RNA-binding protein RBM24 is required for sarcomere assembly and heart contractility. Cardiovasc. Res. *94*, 418–427.
Rauch, J. N., and Gestwicki, J. E. (2014). Binding of Human Nucleotide Exchange Factors to Heat Shock Protein 70 (Hsp70) Generates Functionally Distinct Complexes in Vitro. J. Biol. Chem. *289*, 1402–1414.
Rauch, J. N., Tse, E., Freilich, R., Mok, S.-A., Makley, L. N., Southworth, D. R., and Gestwicki, J. E. (2017). BAG3 Is a Modular, Scaffolding Protein that physically Links Heat Shock Protein 70 (Hsp70) to the Small Heat Shock Proteins. J. Mol. Biol. *429*, 128–141.
Rognoni, L., Stigler, J., Pelz, B., Ylänne, J., and Rief, M. (2012). Dynamic force sensing of filamin revealed in single-molecule experiments. Proc. Natl. Acad. Sci. U. S. A. *109*, 19679–19684.
Ruparelia, A. A., Oorschot, V., Vaz, R., Ramm, G., and Bryson-Richardson, R. J. (2014). Zebrafish models of BAG3 myofibrillar myopathy suggest a toxic gain of function leading to BAG3 insufficiency. Acta Neuropathol. *128*, 821–833.
Schänzer, A. *et al.* (2018). Dysregulated autophagy in restrictive cardiomyopathy due to Pro209Leu mutation in BAG3. Mol. Genet. Metab. *123*, 388–399.
Selcen, D., Muntoni, F., Burton, B. K., Pegoraro, E., Sewry, C., Bite, A., and Engel, A. G. (2009). Mutation in BAG3 causes severe dominant childhood muscular dystrophy. Ann. Neurol. *65*, 83–89.
Sharif, A. A. D., and Hergovich, A. (2018). The NDR/LATS protein kinases in immunology and cancer biology. Semin. Cancer Biol. *48*, 104–114.
Sowa, M. E., Bennett, E. J., Gygi, S. P., and Harper, J. W. (2009). Defining the Human Deubiquitinating Enzyme Interaction Landscape. Cell *138*, 389–403.
Tamaskovic, R., Bichsel, S. J., Rogniaux, H., Stegert, M. R., and Hemmings, B. A. (2003). Mechanism of Ca2+-mediated Regulation of NDR Protein Kinase through Autophosphorylation and Phosphorylation by an Upstream Kinase. J. Biol. Chem.

278, 6710–6718.

Tang, F. *et al.* (2015). The kinases NDR1/2 act downstream of the Hippo homolog MST1 to mediate both egress of thymocytes from the thymus and lymphocyte motility. Sci. Signal. *8*, ra100-ra100.

Ulbricht, A. *et al.* (2013). Cellular mechanotransduction relies on tension-induced and chaperone-assisted autophagy. Curr. Biol. *23*, 430–435.

Ulbricht, A., Gehlert, S., Leciejewski, B., Schiffer, T., Bloch, W., and Höhfeld, J. (2015). Induction and adaptation of chaperone-assisted selective autophagy CASA in response to resistance exercise in human skeletal muscle. Autophagy *11*, 538–546.

Vichalkovski, A., Gresko, E., Cornils, H., Hergovich, A., Schmitz, D., and Hemmings, B. A. (2008). NDR Kinase Is Activated by RASSF1A/MST1 in Response to Fas Receptor Stimulation and Promotes Apoptosis. Curr. Biol. *18*, 1889–1895.

Wackerhage, H., Del Re, D. P., Judson, R. N., Sudol, M., and Sadoshima, J. (2014). The Hippo signal transduction network in skeletal and cardiac muscle. Sci. Signal. *7*, re4-re4.

Wilkinson, D. S. *et al.* (2015). Phosphorylation of LC3 by the Hippo Kinases STK3/STK4 Is Essential for Autophagy. Mol. Cell *57*, 55–68.

Winklhofer, K. F. (2014). Parkin and mitochondrial quality control: toward assembling the puzzle. Trends Cell Biol. *24*, 332–341.

Wrighton, K. H. (2011). Mechanotransduction: YAP and TAZ feel the force. Nat. Rev. Mol. Cell Biol. *12*, 404.

Wu, Z., Sawada, T., Shiba, K., Liu, S., Kanao, T., Takahashi, R., Hattori, N., Imai, Y., and Lu, B. (2013). Tricornered/NDR kinase signaling mediates PINK1-directed mitochondrial quality control and tissue maintenance. Genes Dev. *27*, 157–162.

Yang, J., Hung, L.-H., Licht, T., Kostin, S., Looso, M., Khrameeva, E., Bindereif, A., Schneider, A., and Braun, T. (2014). RBM24 Is a Major Regulator of Muscle-Specific Alternative Splicing. Dev. Cell *31*, 87–99.

Yorimitsu, T., and Klionsky, D. J. (2005). Autophagy: molecular machinery for self-eating. Cell Death Differ *12 Suppl 2*, 1542–1552.

Yu, F.-X., and Guan, K.-L. (2013). The Hippo pathway: regulators and regulations. Genes Dev. *27*, 355–371.

Zhang, L. *et al.* (2015). NDR Functions as a Physiological YAP1 Kinase in the Intestinal Epithelium. Curr. Biol. *25*, 296–305.

FIGURE LEGENDS

FIGURE 1: The CASA-mediating cochaperone BAG3 interacts with STK38. (A) Schematic presentation of the CASA pathway. (UBC - ubiquitin conjugating enzyme, ub - ubiquitin) (B) STK38 was detectable in endogenous BAG3 complexes isolated from A7r5 cells by immunoprecipitation (IP) with an anti-BAG3 antibody (α-BAG3). A control sample received unrelated rabbit IgGs (IgG). Ex. corresponds to 40 µg protein of the cell extract. Indicated proteins were detected by western blotting with corresponding antibodies. (C) Schematic presentation of the domain structure of STK38. The lysine at position 118 (K118) is essential for the kinase activity of STK38. Phosphorylation of threonine 444 (T444) by upstream kinases activates STK38. (D) BAG3 directly binds to the carboxy-terminus of STK38. Purified BAG3 (0.4 µM) was incubated with 2 µM of MBP or MBP-STK38 fusion proteins, followed by isolation on an amylose resin. 10% of each sample was analyzed by western blotting. Indicated proteins were detected with an anti-MBP and anti-BAG3 antibody, respectively. (See also Supplemental Table S1.)

FIGURE 2: STK38 inhibits BAG3-mediated autophagy. (A) Depletion of STK38 facilitates the degradation of filamin. A7r5 cells were transiently transfected for 72 h with siRNA directed against STK38 (siSTK38). Control cells received allstars negative control siRNA (control). 24 h before lysis cells were transferred to fibronectin-coated culture dishes. When indicated, cells were incubated with cycloheximide (50 µM) for 16 h. 50 µg protein were loaded per lane. Filamin and γ-tubulin were detected by western blotting with corresponding antibodies. Signal intensities were quantified by densitometry, whereby the filamin level was normalized to the level of γ-tubulin detected in the same sample. Filamin level in control cells was set to 1. Data represent mean values +/- SEM: $n \geq 16$, $^{*}p \leq 0.05$, $^{***}p \leq 0.001$. (B) STK38 was depleted in A7r5 cells transiently transfected with a corresponding siRNA (siSTK38) for 72 h. Control cells received allstars negative control siRNA (control). 50 µg protein were loaded per lane. Indicated proteins were detected by western blotting with corresponding antibodies. (C) Depletion of STK38 stimulates the autophagic degradation of SYNPO2 in adherent A7r5 cells. A7r5 cells were transiently transfected for 48 h with siRNA directed against STK38 (siSTK38). Control cells received allstars negative control siRNA (control). Treatment with chloroquine (100

µM) was performed for 16 h prior to lysis (CQ). When indicated, cells were incubated with cycloheximide (50 µM) for 1, 2 or 3 h before lysis. 50 µg protein were loaded per lane. Isoforms a, b and c of SYNPO2 and γ-tubulin were detected by western blotting with corresponding antibodies. Signal intensities were quantified, whereby the level of SYNPO2 isoforms was normalized to the level of γ-tubulin detected in the same sample. (D) Quantification of the data presented in (C). Level of SYNPO2 isoforms detected in control cells at time point 0 was set to 1. Data represent mean values +/- SEM: n ≥ 5. (E) Overexpression of STK38 and the kinase-dead variant STK38-K118R inhibits the degradation of filamin in adherent smooth muscle cells. A7r5 cells were transiently transfected with plasmids encoding STK38 and STK38-K118R for 72 h. Control cells received empty vector. 24 h before lysis cells were transferred to fibronectin-coated culture dishes. When indicated, cells were incubated with cycloheximide (50 µM) for 16 h. 50 µg protein were loaded per lane. Filamin, STK38 and γ-tubulin were detected by western blotting with corresponding antibodies. Signal intensities were quantified, whereby the filamin level was normalized to the level of γ-tubulin detected in the same sample or to the protein amount determined by SDS-PAGE and Ponceau S staining. Filamin level in control cells was set to 1. Data represent mean values +/- SEM: n ≥ 15, *p ≤ 0.05, **p ≤ 0.01, ***p ≤ 0.001. (F) STK38 expression is induced in murine myotubes subjected to prolonged mechanical stress and induction correlates with an attenuation of filamin degradation. Differentiated C2C12 myotubes were subjected to electrical pulse stimulation (EPS) for the indicated times, followed by lysis and western blotting. 60 µg protein were loaded per lane. Indicated proteins were detected using specific antibodies. (G) Quantification of the data presented in (F). Level of indicated proteins detected at time point 0 was set to 1. Data represent mean values +/- SEM: n ≥ 4.

FIGURE 3: Hippo kinases that act upstream of STK38 contribute to the regulation of CASA. (A) A7r5 cells were transiently transfected with siRNAs directed against STK3, STK4 and STK24 for 48 h. Control cells received allstars negative control siRNA (control). Transcript levels were determined by quantitative real time PCR. Data represent mean values +/- SEM: n = 3. (B) Depletion of STK3 and STK4 attenuates SYNPO2 degradation, whereas depletion of STK24 facilitates turnover. A7r5 cells were transiently transfected for 48 h with siRNA directed against the indicated kinases. Control cells received allstars negative control siRNA (control).

When indicated, cells were incubated with cycloheximide (50 µM) for 3 h before lysis. 60 µg protein were loaded per lane. Isoforms a, b and c of SYNPO2 and γ-tubulin were detected by western blotting with corresponding antibodies. Signal intensities were quantified and normalized to the level of γ-tubulin or total protein detected in the same sample. SYNPO2 level in control cells, which did not receive cycloheximide, was set to 1. Data represent mean values +/- SEM: n ≥ 10, *p ≤ 0.05, **p ≤ 0.01. (C) Depletion of STK24 facilitates the degradation of filamin. A7r5 cells were transiently transfected for 72 h with siRNA directed against STK24 (siSTK24) or control siRNA (control). 24 h before lysis cells were transferred to fibronectin-coated culture dishes. When indicated, cells were incubated with cycloheximide (50 µM) for 16 h. 50 µg protein were loaded per lane. Filamin and γ-tubulin were detected by western blotting with corresponding antibodies. Signal intensities were quantified by densitometry, whereby the filamin level was normalized to the level of γ-tubulin detected in the same sample. Filamin level in control cells was set to 1. Data represent mean values +/- SEM: n ≥ 15, *p ≤ 0.05, ***p ≤ 0.001. (D) Overexpression of STK38-T444A, which cannot be phosphorylated by STK38 upstream kinases, does not significantly affect filamin degradation. A7r5 cells were transiently transfected with plasmids encoding STK38 and STK38-T444A for 72 h. Control cells received empty vector. 24 h before lysis cells were transferred to fibronectin-coated culture dishes. When indicated, cells were incubated with cycloheximide (50 µM) for 16 h. 50 µg protein were loaded per lane. Filamin, STK38 and γ-tubulin were detected by western blotting with corresponding antibodies. Signal intensities were quantified, whereby the filamin level was normalized to the level of γ-tubulin detected in the same sample. Filamin level in control cells was set to 1. Data represent mean values +/- SEM: n ≥ 6, *p ≤ 0.05, **p ≤ 0.01, ***p ≤ 0.001. (E) STK38-T444A displays reduced affinity for BAG3. HeLa cells were transiently transfected with plasmids encoding FLAG-BAG3, HA-STK38, HA-STK38-K118R and HA-STK38-T444A as indicated for 48 h, followed by immunoprecipitation with an anti-FLAG antibody resin (α-FLAG IP). Immunoprecipitated complexes were analyzed by western blotting using specific antibodies. Ex. corresponds to 50 µg protein of the cell lysates. (F) Quantification of data obtained under (E). STK38 level detected in BAG3 complexes was set to 1. Data represent mean values +/- SEM: n ≥ 5, *p ≤ 0.05, **p ≤ 0.01, ***p ≤ 0.001.

FIGURE 4: CASA proceeds independently of BECN1 and RALB. (A) BECN1 and RALB were depleted in A7r5 cells transiently transfected with corresponding siRNAs for 72 h. Control cells received allstars negative control siRNA (control). 50 µg protein were loaded per lane. Indicated proteins were detected by western blotting with corresponding antibodies. (B) SYNPO2 degradation is not affected by depletion of BECN1 or RALB in adherent smooth muscle cells. A7r5 cells were transiently transfected for 72 h with siRNA directed against the indicated proteins. Control cells received allstars negative control siRNA (control). When indicated, cells were incubated with cycloheximide (50 µM) for 4 h before lysis. 60 µg protein were loaded per lane. SYNPO2 isoforms and γ-tubulin were detected by western blotting with corresponding antibodies. Signal intensities were quantified, whereby the level of SYNPO2 isoforms was normalized to the level of γ-tubulin detected in the same sample. SYNPO2 level in control cells, which did not receive cycloheximide, was set to 1. Data represent mean values +/- SEM: n ≥ 4. (n.s. - not significant). (C) Depletion of BECN1 and RALB does not affect the degradation of filamin in adherent A7r5 cells. A7r5 cells were transiently transfected for 72 h with siRNA directed against RALB (siRALB), BECN1 (siBECN1) or control siRNA (control). 24 h before lysis cells were transferred to fibronectin-coated culture dishes. When indicated, cells were incubated with cycloheximide (50 µM) for 16 h. 50 µg protein were loaded per lane. Filamin and γ-tubulin were detected by western blotting with corresponding antibodies. Signal intensities were quantified by densitometry, whereby the filamin level was normalized to the level of γ-tubulin detected in the same sample. Filamin level in control cells was set to 1. Data represent mean values +/- SEM: n ≥ 13 (n.s. - not significant).

FIGURE 5: STK38 disrupts the interaction of BAG3 with HSPB8 and SYNPO2 in a manner independent of its kinase activity. (A) Association of STK38 with BAG3 interferes with the binding of the cochaperone to HSPB8. HeLa cells were transiently transfected with plasmids encoding FLAG-BAG3, HA-STK38 and HA-STK38-K118R as indicated for 48 h, followed by immunoprecipitation with an anti-FLAG antibody resin (α-FLAG IP). Isolated complexes were treated with ATP (ATP) prior to elution with glycine containing buffer (glycine). Indicated proteins were detected by western blotting using specific antibodies. Input corresponds to 50 µg protein of the cell lysates. (B) Overexpression of STK38 or the kinase-dead variant STK38-K118R in

A7r5 cells disrupts the interaction of SYNPO2a with BAG3. HeLa cells were transiently transfected with plasmids encoding SYNPO2a, STK38 and STK38-K118R as indicated for 48 h, followed by immunoprecipitation with an anti-SYNPO2 antibody (α-SYNPO2). Control samples received unrelated rabbit IgGs (IgG) instead. Indicated proteins were detected by western blotting using specific antibodies. Input corresponds to 50 µg protein of the cell lysates. (C) STK38 acts as a central switch during protein homeostasis in mammalian cells. It positively regulates mitophagy and starvation- and detachment-induced autophagy through BECN1 and RALB, whereas STK38 inhibits CASA through association with BAG3. Stimulation of cytoskeleton assembly relies on the activation of RBM24 by STK38.

Klimek et al. Figure 1

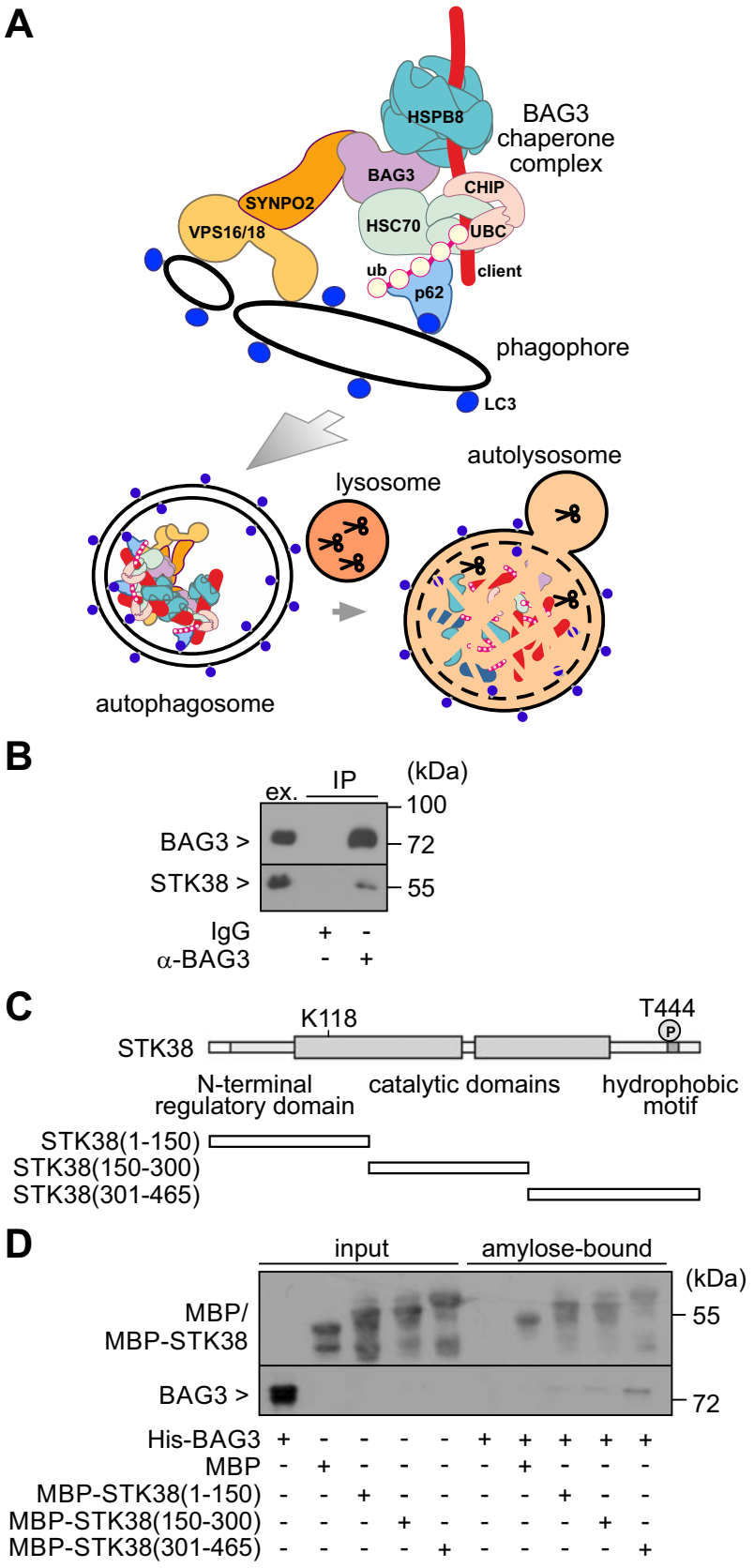

Klimek et al. Figure 2

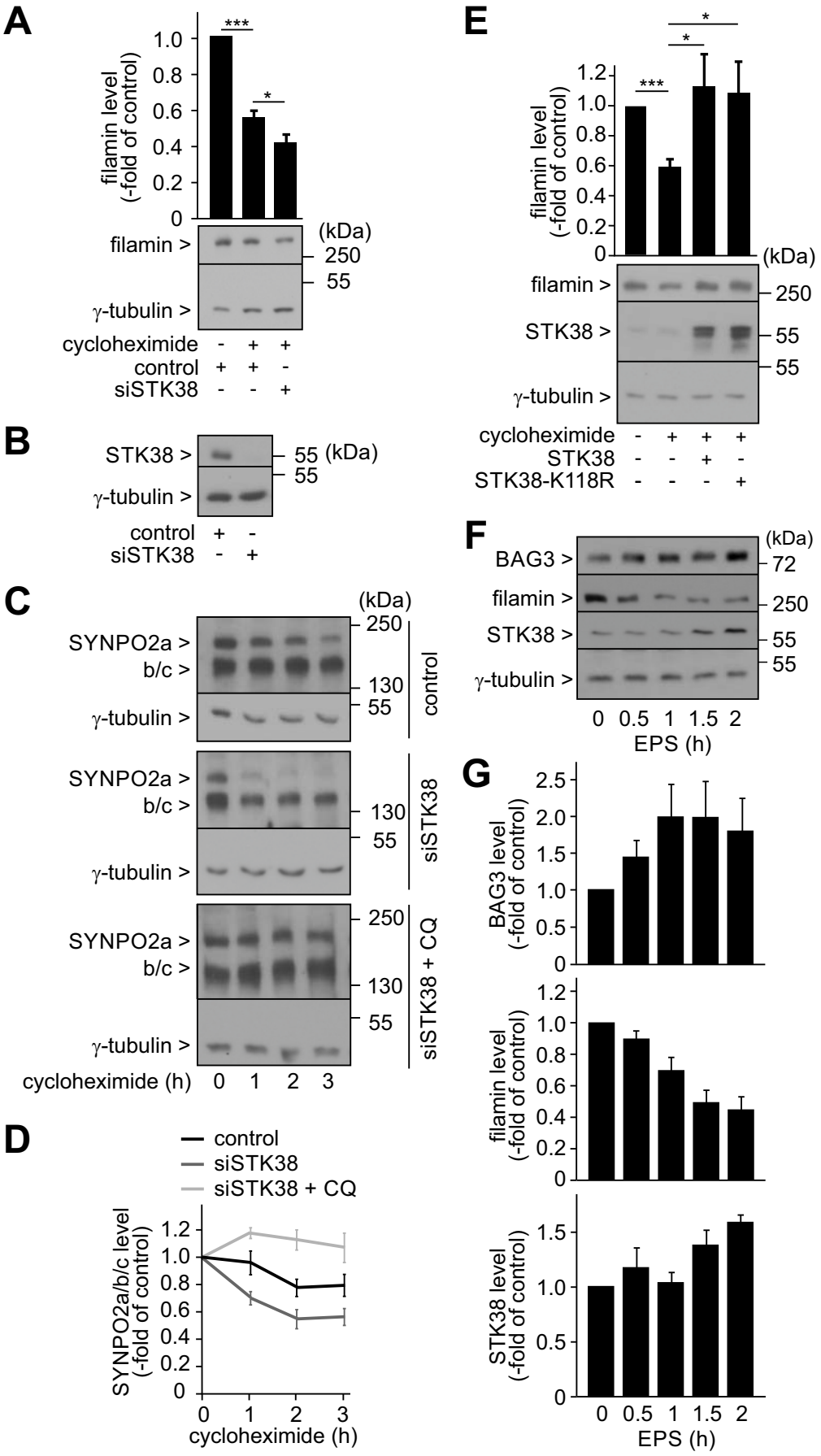

Klimek et al. Figure 3

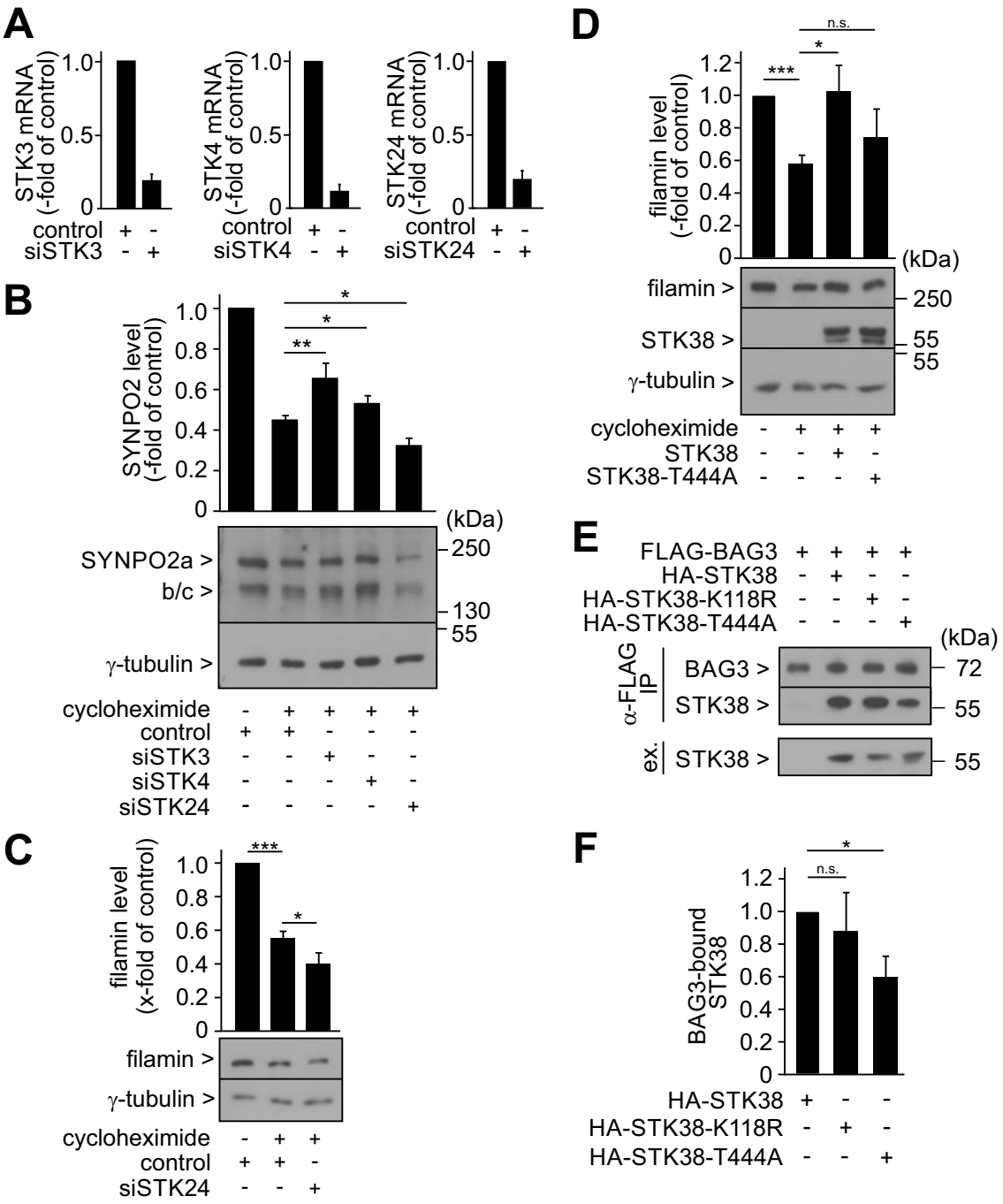

Klimek et al. Figure 4

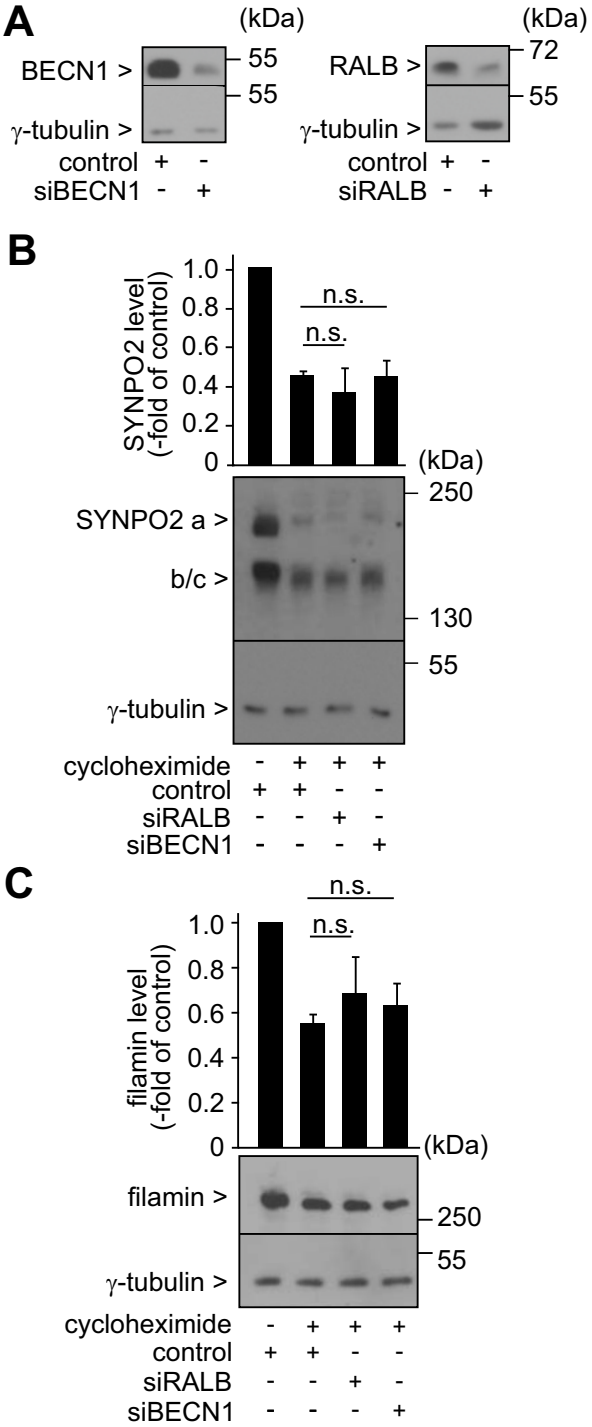

Klimek et al. Figure 5

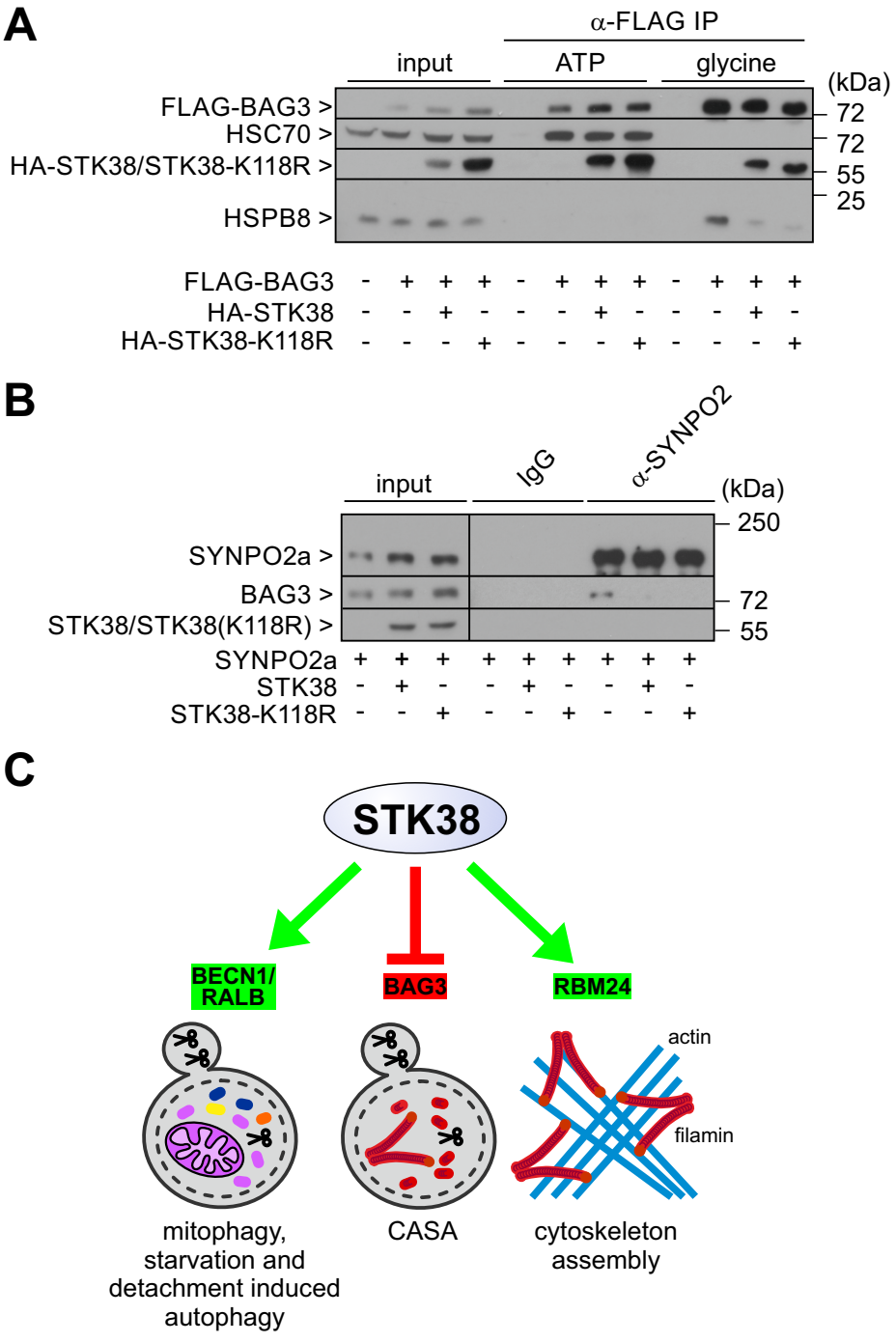

Supplemental Table S1. (Related to Figure 1) Proteomic characterization of BAG3 complexes isolated from HEK293T cells stably expressing N-terminally HA-tagged BAG3.

APSM stands for "average protein spectral matches" and takes into account peptides which match more than one protein in the database.

NDW stands for „normalized weighted D (WD^N) score" and reports the frequency, abundance and reproducibility of each interaction.

GeneID	Symbol	Ave. APSM	NWD	Z	Ratio	Found_in	
9531	BAG3	130	2.66	9.85	8/99	2	bait
11164	NUDT5	3	2.32	9.90	1/99	2	
1856	DVL2	3	2.32	9.90	1/99	2	
9061	PAPSS1	2	1.90	9.90	1/99	2	
6238	RRBP1	2	1.90	9.90	1/99	2	
9255	AIMP1	1	1.34	9.90	1/99	2	
2632	GBE1	1	1.34	9.90	1/99	2	
81875	ISG20L2	1	1.34	9.90	1/99	2	
5784	PTPN14	1	1.34	9.90	1/99	2	
8079	MLF2	1	1.34	9.90	1/99	2	
8602	NOP14	1	1.34	9.90	1/99	2	
84858	ZNF503	1	1.34	9.90	1/99	2	
26353	HSPB8	1	1.34	9.90	1/99	2	BAG3-bdg. sHSP
9054	NFS1	1	1.34	9.90	1/99	2	
573	BAG1	1	1.34	9.90	1/99	2	
9260	PDLIM7	1	1.34	9.90	1/99	2	
10611	PDLIM5	2	0.19	9.90	1/99	1	
11329	STK38	1	0.13	9.90	1/99	1	Hippo network
10787	NCKAP1	1	0.13	9.90	1/99	1	
7259	TSPYL1	1	0.13	9.90	1/99	1	
127018	LYPLAL1	1	0.13	9.90	1/99	1	
26010	SPATS2L	1	0.13	9.90	1/99	1	
24144	TFIP11	1	0.13	9.90	1/99	1	
84524	ZC3H8	1	0.13	9.90	1/99	1	
22930	RAB3GAP1	1	0.13	9.90	1/99	1	
25822	DNAJB5	1	0.13	9.90	1/99	1	
26048	ZNF500	1	0.13	9.90	1/99	1	
79657	RPAP3	1	0.13	9.90	1/99	1	
64975	MRPL41	1	0.13	9.90	1/99	1	
55740	ENAH	1	0.13	9.90	1/99	1	
55835	CENPJ	1	0.13	9.90	1/99	1	
57644	MYH7B	1	0.13	9.90	1/99	1	
10199	MPHOSPH	1	0.13	9.90	1/99	1	
9871	SEC24D	1	0.13	9.90	1/99	1	
2072	ERCC4	1	0.13	9.90	1/99	1	
7913	DEK	1	0.13	9.90	1/99	1	
8027	STAM	1	0.13	9.90	1/99	1	
10813	UTP14A	1	0.13	9.90	1/99	1	
4802	NFYC	1	0.13	9.90	1/99	1	
11222	MRPL3	1	0.13	9.90	1/99	1	
231	AKR1B1	1	0.13	9.90	1/99	1	
359948	IRF2BP2	1	0.13	9.90	1/99	1	
2098	ESD	1	0.13	9.90	1/99	1	
51642	MRPL48	1	0.13	9.90	1/99	1	
196441	ZFC3H1	1	0.13	9.90	1/99	1	
904	CCNT1	1	0.13	9.90	1/99	1	
51010	EXOSC3	1	0.13	9.90	1/99	1	
2037	EPB41L2	1	0.13	9.90	1/99	1	
55086	CXorf57	1	0.13	9.90	1/99	1	

11196	SEC23IP	1	0.13	9.90	1/99	1
56941	C3orf37	1	0.13	9.90	1/99	1
51015	ISOC1	1	0.13	9.90	1/99	1
23644	EDC4	1	0.13	9.90	1/99	1
5987	TRIM27	1	0.13	9.90	1/99	1
79050	NOC4L	1	0.13	9.90	1/99	1
YV012_HU	YV012_HU	1	0.13	9.90	1/99	1
54870	QRICH1	1	0.13	9.90	1/99	1
55269	PSPC1	1	0.13	9.90	1/99	1
26278	SACS	1	0.13	9.90	1/99	1
55003	PAK1IP1	1	0.13	9.90	1/99	1
6241	RRM2	1	0.13	9.90	1/99	1
55749	CCAR1	1	0.13	9.90	1/99	1
80762	NDFIP1	1	0.13	9.90	1/99	1
11080	DNAJB4	1	0.13	9.90	1/99	1
58513	EPS15L1	1	0.13	9.90	1/99	1
5690	PSMB2	1	0.13	9.90	1/99	1
1795	DOCK3	1	0.13	9.90	1/99	1
64067	NPAS3	1	0.13	9.90	1/99	1
91748	C14orf43	1	0.13	9.90	1/99	1
7088	TLE1	1	0.13	9.90	1/99	1
2021	ENDOG	1	0.13	9.90	1/99	1
51684	SUFU	1	0.13	9.90	1/99	1
404672	GTF2H5	1	0.13	9.90	1/99	1
284403	WDR62	1	0.13	9.90	1/99	1
200081	TXLNA	1	0.13	9.90	1/99	1
23558	WBP2	11	1.97	9.79	3/99	2
55833	UBAP2	4	0.89	9.38	3/99	2
8209	C21orf33	3	1.16	9.25	2/99	2
9898	UBAP2L	8	0.52	9.10	9/99	2
10762	NUP50	2	0.95	8.95	2/99	2
760	CA2	2	0.95	8.95	2/99	2
1266	CNN3	2	0.13	8.95	2/99	1
28988	DBNL	2	0.13	8.95	2/99	1
817	CAMK2D	3	0.77	8.94	3/99	2
51645	PPIL1	3	0.77	8.94	3/99	2
10049	DNAJB6	5	0.30	8.53	10/99	2
7812	CSDE1	9	0.21	8.50	22/99	2
2010	EMD	2	0.63	8.17	3/99	2
64746	ACBD3	2	0.63	8.17	3/99	2
80335	WDR82	2	0.63	8.17	3/99	2
23008	KLHDC10	2	0.63	8.17	3/99	2
10181	RBM5	2	0.11	8.17	3/99	1
27044	SND1	3	0.46	8.14	5/99	2
3337	DNAJB1	2	0.47	7.50	4/99	2
136319	MTPN	2	0.47	7.50	4/99	2
253943	YTHDF3	2	0.47	7.50	4/99	2
10250	SRRM1	5	0.20	7.48	15/99	2
84295	PHF6	1	0.67	7.00	2/99	2
8220	DGCR14	1	0.67	7.00	2/99	2

8812	CCNK	1	0.10	7.00	2/99	1
115708	TRMT61A	1	0.10	7.00	2/99	1
4678	NASP	1	0.10	7.00	2/99	1
5294	PIK3CG	1	0.10	7.00	2/99	1
7175	TPR	1	0.10	7.00	2/99	1
27107	ZBTB11	1	0.10	7.00	2/99	1
7384	UQCRC1	1	0.10	7.00	2/99	1
83889	WDR87	1	0.10	7.00	2/99	1
51163	DBR1	1	0.10	7.00	2/99	1
23215	PRRC2C	1	0.10	7.00	2/99	1
1891	ECH1	1	0.10	7.00	2/99	1
1155	TBCB	1	0.10	7.00	2/99	1
10540	DCTN2	1	0.10	7.00	2/99	1
10248	POP7	1	0.10	7.00	2/99	1
1371	CPOX	1	0.10	7.00	2/99	1
55339	WDR33	1	0.10	7.00	2/99	1
10097	ACTR2	1	0.10	7.00	2/99	1
984	CDK11B	1	0.10	7.00	2/99	1
4677	NARS	1	0.10	7.00	2/99	1
2539	G6PD	1	0.10	7.00	2/99	1
90678	LRSAM1	1	0.10	7.00	2/99	1
991	CDC20	1	0.10	7.00	2/99	1
79833	GEMIN6	1	0.10	7.00	2/99	1
1650	DDOST	1	0.10	7.00	2/99	1
1211	CLTA	2	0.38	6.93	5/99	2
6829	SUPT5H	2	0.38	6.93	5/99	2
9747	FAM115A	3	0.26	6.55	9/99	2
84271	POLDIP3	2	0.63	6.50	3/99	2
6711	SPTBN1	4	0.18	6.44	15/99	2
5356	PLRG1	2	0.27	6.19	7/99	2
7916	PRRC2A	4	1.34	6.11	2/99	2
705	BYSL	2	0.24	5.97	8/99	2
11315	PARK7	2	0.24	5.97	8/99	2
9631	NUP155	2	0.24	5.97	8/99	2
1466	CSRP2	1	0.45	5.71	3/99	2
8407	TAGLN2	1	0.45	5.71	3/99	2
55660	PRPF40A	1	0.08	5.71	3/99	1
286077	FAM83H	1	0.08	5.71	3/99	1
7385	UQCRC2	1	0.08	5.71	3/99	1
6311	ATXN2	1	0.08	5.71	3/99	1
51068	NMD3	1	0.08	5.71	3/99	1
29088	MRPL15	1	0.08	5.71	3/99	1
1793	DOCK1	1	0.08	5.71	3/99	1
10015	PDCD6IP	1	0.08	5.71	3/99	1
64282	PAPD5	1	0.08	5.71	3/99	1
83443	SF3B5	1	0.08	5.71	3/99	1
54039	PCBP3	2	0.32	5.65	6/99	2
5686	PSMA5	2	0.27	5.46	7/99	2
9632	SEC24C	4	0.09	5.34	29/99	2
92140	MTDH	2	0.63	5.24	3/99	2

5976	UPF1	5	0.12	5.19	26/99	2	
22872	SEC31A	3	0.15	4.96	16/99	2	
1615	DARS	2	0.15	4.89	13/99	2	
58517	RBM25	1	0.34	4.80	4/99	2	
3376	IARS	1	0.34	4.80	4/99	2	
3796	KIF2A	1	0.34	4.80	4/99	2	
57696	DDX55	1	0.07	4.80	4/99	1	
10539	GLRX3	1	0.07	4.80	4/99	1	
23211	ZC3H4	1	0.07	4.80	4/99	1	
1479	CSTF3	1	0.07	4.80	4/99	1	
29889	GNL2	1	0.07	4.80	4/99	1	
6603	SMARCD2	1	0.07	4.80	4/99	1	
11331	PHB2	1	0.07	4.80	4/99	1	
6173	RPL36A	1	0.07	4.80	4/99	1	
54464	XRN1	1	0.07	4.80	4/99	1	
10061	ABCF2	1	0.07	4.80	4/99	1	
54552	GNL3L	1	0.07	4.80	4/99	1	
339230	CCDC137	1	0.07	4.80	4/99	1	
6240	RRM1	1	0.07	4.80	4/99	1	
29894	CPSF1	2	0.14	4.74	14/99	2	
5631	PRPS1	2	0.63	4.71	3/99	2	
5217	PFN2	2	0.12	4.46	16/99	2	
1781	DYNC1I2	1	0.10	4.41	2/99	1	
29110	TBK1	1	0.10	4.41	2/99	1	
226	ALDOA	1	0.27	4.32	5/99	2	
80222	TARS2	1	0.06	4.32	5/99	1	
9738	CP110	1	0.06	4.32	5/99	1	
8568	RRP1	1	0.06	4.32	5/99	1	
23028	KDM1A	1	0.06	4.32	5/99	1	
31	ACACA	1	0.06	4.32	5/99	1	
79724	ZNF768	1	0.06	4.32	5/99	1	
9669	EIF5B	1	0.06	4.32	5/99	1	
10273	STUB1	8	0.24	4.25	16/99	2	CHIP
388697	HRNR	2	0.21	4.25	9/99	2	
79869	CPSF7	2	0.16	4.20	12/99	2	
51154	MRTO4	2	0.10	4.19	19/99	2	
9532	BAG2	7	0.08	4.15	42/99	2	
654483	BOLA2B	2	0.12	4.14	16/99	2	
6709	SPTAN1	4	0.07	4.13	38/99	2	
7112	TMPO	1	0.08	4.00	3/99	1	
65003	MRPL11	1	0.06	3.92	6/99	1	
23234	DNAJC9	1	0.06	3.92	6/99	1	
8872	CDC123	1	0.06	3.92	6/99	1	
223	ALDH9A1	1	0.06	3.92	6/99	1	
26608	TBL2	1	0.06	3.92	6/99	1	
2017	CTTN	1	0.06	3.92	6/99	1	
2058	EPRS	2	0.12	3.85	16/99	2	
26284	ERAL1	2	0.05	3.85	16/99	1	
5394	EXOSC10	4	0.14	3.83	19/99	2	
6165	RPL35A	3	0.05	3.77	51/99	2	

7307	U2AF1	2	0.09	3.67	22/99	2
1823	DSC1	1	0.07	3.65	4/99	1
65109	UPF3B	1	0.05	3.58	7/99	1
54865	GPATCH4	1	0.05	3.58	7/99	1
54512	EXOSC4	1	0.05	3.58	7/99	1
200916	RPL22L1	1	0.05	3.58	7/99	1
3066	HDAC2	2	0.21	3.56	9/99	2
10992	SF3B2	2	0.11	3.44	17/99	2
23451	SF3B1	5	0.12	3.42	25/99	2
5688	PSMA7	1	0.17	3.41	8/99	2
4191	MDH2	1	0.05	3.41	8/99	1
55173	MRPS10	1	0.05	3.41	8/99	1
64783	RBM15	1	0.05	3.41	8/99	1
348262	FAM195B	1	0.05	3.41	8/99	1
3654	IRAK1	1	0.05	3.41	8/99	1
56829	ZC3HAV1	2	0.11	3.36	18/99	2
829	CAPZA1	1	0.06	3.36	5/99	1
1936	EEF1D	2	0.17	3.33	11/99	2
10606	PAICS	3	0.11	3.33	22/99	2
55692	LUC7L	1	0.22	3.21	6/99	2
56252	YLPM1	1	0.06	3.21	6/99	1
6123	RPL3L	1	0.06	3.21	6/99	1
10484	SEC23A	8	0.05	3.21	79/99	2
83640	FAM103A1	3	0.07	3.20	34/99	2
2547	XRCC6	7	0.10	3.18	35/99	2
4144	MAT2A	2	0.09	3.15	22/99	2
26993	AKAP8L	1	0.15	3.14	9/99	2
23016	EXOSC7	1	0.04	3.14	9/99	1
55907	CMAS	1	0.04	3.14	9/99	1
23560	GTPBP4	3	0.12	3.13	19/99	2
7266	DNAJC7	5	0.12	3.11	26/99	2
9529	BAG5	1	0.07	3.03	4/99	1
9939	RBM8A	1	0.07	3.03	4/99	1
8894	EIF2S2	1	0.13	3.00	10/99	2
23185	LARP4B	1	0.04	3.00	10/99	1
10179	RBM7	1	0.04	3.00	10/99	1
6923	TCEB2	1	0.19	2.97	7/99	2
740	MRPL49	1	0.05	2.97	7/99	1
160	AP2A1	1	0.45	2.88	3/99	2
79672	FN3KRP	1	0.05	2.84	8/99	1
58477	SRPRB	1	0.05	2.84	8/99	1
5478	PPIA	3	0.07	2.82	35/99	2
1019	CDK4	3	0.15	2.78	16/99	2
7536	SF1	1	0.12	2.78	11/99	2
55596	ZCCHC8	1	0.04	2.78	11/99	1
51504	TRMT112	1	0.04	2.78	11/99	1
11335	CBX3	1	0.34	2.76	4/99	2
1937	EEF1G	3	0.04	2.74	55/99	2
4288	MKI67	1	0.04	2.73	9/99	1
F5H428_H	F5H428_H	1	0.04	2.73	9/99	1

55920	RCC2	4	0.07	2.72	36/99	2
6050	RNH1	1	0.06	2.71	6/99	1
3028	HSD17B10	4	0.09	2.69	33/99	2
2926	GRSF1	3	0.06	2.68	36/99	2
51373	MRPS17	1	0.11	2.67	12/99	2
81	ACTN4	1	0.04	2.67	12/99	1
5813	PURA	1	0.04	2.67	12/99	1
84309	NUDT16L1	1	0.04	2.67	12/99	1
84310	C7orf50	2	0.08	2.62	23/99	2
51096	UTP18	1	0.06	2.58	5/99	1
2023	ENO1	3	0.07	2.57	31/99	2
6117	RPA1	1	0.04	2.56	13/99	1
57647	DHX37	1	0.04	2.54	10/99	1
84946	LTV1	1	0.04	2.54	10/99	1
10657	KHDRBS1	3	0.05	2.53	49/99	2
6208	RPS14	6	0.04	2.48	88/99	2
5431	POLR2B	4	0.09	2.47	30/99	2
55421	C17orf85	1	0.04	2.46	14/99	1
7317	UBA1	3	0.21	2.44	13/99	2
83473	KATNAL2	1	0.04	2.41	9/99	1
114034	TOE1	1	0.05	2.39	7/99	1
54460	MRPS21	1	0.05	2.39	7/99	1
27339	PRPF19	4	0.05	2.38	49/99	2
3692	EIF6	1	0.04	2.35	12/99	1
8985	PLOD3	1	0.04	2.35	12/99	1
5437	POLR2H	1	0.04	2.35	12/99	1
10940	POP1	2	0.11	2.34	18/99	2
59	ACTA2	3	0.26	2.33	9/99	2
5936	RBM4	1	0.17	2.31	8/99	2
51202	DDX47	1	0.05	2.31	8/99	1
3315	HSPB1	2	0.24	2.29	8/99	2
7520	XRCC5	6	0.10	2.28	34/99	2
5110	PCMT1	2	0.05	2.26	41/99	2
1968	EIF2S3	1	0.04	2.26	13/99	1
5434	POLR2E	1	0.04	2.26	13/99	1
2879	GPX4	1	0.08	2.24	3/99	1
3310	HSPA6	25	0.07	2.24	94/99	2
283742	FAM98B	2	0.05	2.23	36/99	2
8731	RNMT	3	0.06	2.22	36/99	2
5928	RBBP4	2	0.04	2.18	45/99	2
51441	YTHDF2	1	0.03	2.18	17/99	1
3836	KPNA1	1	0.11	2.15	12/99	2
11273	ATXN2L	2	0.47	2.11	4/99	2
11091	WDR5	1	0.03	2.10	15/99	1
832	CAPZB	1	0.34	2.09	4/99	2
1029	CDKN2A	2	0.08	2.09	25/99	2
83737	ITCH	1	0.06	2.09	5/99	1
6421	SFPQ	2	0.07	2.06	26/99	2
51747	LUC7L3	2	0.07	2.04	27/99	2
5981	RFC1	1	0.08	2.02	16/99	2

10963	STIP1	1	0.06	2.02	5/99	1	
1213	CLTC	24	0.13	2.00	83/99	2	
1965	EIF2S1	2	0.06	2.00	32/99	2	
6158	RPL28	2	0.05	1.99	41/99	2	
6132	RPL8	5	0.04	1.99	84/99	2	
11321	GPN1	1	0.05	1.98	7/99	1	
10483	SEC23B	4	0.10	1.96	28/99	2	
2091	FBL	2	0.05	1.96	41/99	2	
8453	CUL2	1	0.05	1.96	7/99	1	
8289	ARID1A	3	0.07	1.95	33/99	2	
988	CDC5L	4	0.13	1.93	27/99	2	
57690	TNRC6C	1	0.04	1.93	12/99	1	
5432	POLR2C	1	0.04	1.93	13/99	1	
10921	RNPS1	1	0.03	1.93	18/99	1	
8895	CPNE3	1	0.03	1.93	18/99	1	
23350	U2SURP	2	0.05	1.92	41/99	2	
2969	GTF2I	1	0.05	1.89	8/99	1	
81608	FIP1L1	1	0.10	1.87	14/99	2	
57062	DDX24	1	0.04	1.87	13/99	1	
23029	RBM34	1	0.08	1.86	16/99	2	
5985	RFC5	1	0.03	1.86	16/99	1	
6921	TCEB1	1	0.11	1.85	12/99	2	
3839	KPNA3	1	0.04	1.85	12/99	1	
51663	ZFR	1	0.04	1.85	9/99	1	
5859	QARS	1	0.04	1.85	12/99	1	
5917	RARS	1	0.08	1.84	17/99	2	
6598	SMARCB1	1	0.04	1.84	14/99	1	
5393	EXOSC9	1	0.04	1.84	14/99	1	
6427	SRSF2	3	0.03	1.84	67/99	2	
55234	SMU1	1	0.04	1.83	9/99	1	
29896	TRA2A	1	0.03	1.83	23/99	1	
23524	SRRM2	5	0.22	1.82	22/99	2	
3312	HSPA8	98	0.13	1.82	99/99	2	HSC70
10549	PRDX4	5	0.06	1.80	48/99	2	
65993	MRPS34	1	0.04	1.79	13/99	1	
3306	HSPA2	23	0.18	1.78	35/99	2	
1503	CTPS	6	0.06	1.77	63/99	2	
3295	HSD17B4	1	0.04	1.77	13/99	1	
60496	AASDHPPT	1	0.05	1.76	8/99	1	
5430	POLR2A	5	0.08	1.74	42/99	2	
14	AAMP	1	0.04	1.72	10/99	1	
6566	SLC16A1	1	0.03	1.72	16/99	1	
5903	RANBP2	1	0.03	1.72	19/99	1	
65265	C8orf33	1	0.04	1.71	14/99	1	
124801	LSM12	1	0.03	1.70	20/99	1	
10262	SF3B4	1	0.03	1.70	20/99	1	
6732	SRPK1	2	0.04	1.66	26/99	1	
4637	MYL6	1	0.07	1.65	4/99	1	
4841	NONO	3	0.04	1.64	63/99	2	
64848	YTHDC2	2	0.10	1.62	19/99	2	

5518	PPP2R1A	4	0.09	1.60	36/99	2	
3945	LDHB	1	0.03	1.58	18/99	1	
83759	RBM4B	1	0.07	1.57	20/99	2	
4904	YBX1	11	0.05	1.57	88/99	2	
10772	SRSF10	1	0.03	1.57	20/99	1	
9584	RBM39	2	0.05	1.56	42/99	2	
47	ACLY	2	0.07	1.55	27/99	2	
3799	KIF5B	1	0.45	1.54	3/99	2	
11171	STRAP	3	0.03	1.54	46/99	1	
84263	HSDL2	1	0.03	1.51	19/99	1	
10238	DCAF7	1	0.03	1.50	22/99	1	
5479	PPIB	1	0.06	1.49	6/99	1	
9908	G3BP2	3	0.08	1.46	39/99	2	
51602	NOP58	1	0.03	1.46	20/99	1	
6205	RPS11	1	0.03	1.42	27/99	1	
50809	HP1BP3	1	0.03	1.39	20/99	1	
9295	SRSF11	1	0.05	1.37	26/99	2	
79009	DDX50	3	0.10	1.36	24/99	2	
6780	STAU1	2	0.03	1.36	37/99	1	
9588	PRDX6	1	0.06	1.35	21/99	2	
22827	PUF60	2	0.05	1.32	42/99	2	
23243	ANKRD28	1	0.07	1.31	4/99	1	
10155	TRIM28	4	0.04	1.31	60/99	2	
5216	PFN1	1	0.04	1.31	14/99	1	
2312	FLG	1	0.04	1.31	12/99	1	
6206	RPS12	1	0.03	1.31	25/99	1	
10197	PSME3	1	0.17	1.30	8/99	2	
10413	YAP1	1	0.10	1.30	2/99	1	Hippo network
6189	RPS3A	10	0.05	1.30	79/99	2	
90957	DHX57	2	0.07	1.29	28/99	2	
23071	ERP44	1	0.04	1.29	12/99	1	
10970	CKAP4	1	0.04	1.29	10/99	1	
23435	TARDBP	1	0.03	1.28	22/99	1	
3615	IMPDH2	1	0.03	1.26	23/99	1	
57532	NUFIP2	2	0.66	1.25	3/99	2	
23521	RPL13A	3	0.03	1.25	85/99	2	
22803	XRN2	6	0.04	1.22	76/99	2	
7150	TOP1	2	0.07	1.21	29/99	2	
64949	MRPS26	1	0.03	1.20	16/99	1	
9775	EIF4A3	1	0.05	1.19	28/99	2	
8370	HIST2H4A	2	0.05	1.18	42/99	2	
103	ADAR	1	0.03	1.18	22/99	1	
221092	HNRNPUL2	1	0.06	1.16	22/99	2	
5052	PRDX1	9	0.04	1.16	95/99	2	
26135	SERBP1	3	0.04	1.13	55/99	2	
6599	SMARCC1	3	0.04	1.11	54/99	2	
55646	LYAR	2	0.04	1.11	43/99	2	
10270	AKAP8	1	0.03	1.11	26/99	1	
1984	EIF5A	2	0.04	1.10	47/99	2	
6152	RPL24	4	0.03	1.10	91/99	2	

6143	RPL19	3	0.04	1.08	66/99	2	
6227	RPS21	4	0.04	1.07	76/99	2	
27316	RBMX	3	0.04	1.07	58/99	2	
10399	GNB2L1	2	0.05	1.05	40/99	2	
6625	SNRNP70	11	0.05	1.05	98/99	2	
4839	NOP2	4	0.04	1.05	44/99	1	
3276	PRMT1	3	0.04	1.05	65/99	2	
8570	KHSRP	4	0.03	1.05	82/99	2	
8683	SRSF9	1	0.02	1.05	30/99	1	
10482	NXF1	1	0.07	1.04	19/99	2	
5935	RBM3	2	0.03	1.03	58/99	2	
154796	AMOT	3	0.46	1.02	5/99	2	Hippo network
983	CDK1	1	0.06	1.00	7/99	1	
6154	RPL26	2	0.04	1.00	46/99	2	
4670	HNRNPM	12	0.05	0.99	86/99	2	
23076	RRP1B	1	0.05	0.97	25/99	2	
3069	HDLBP	2	0.10	0.96	23/99	2	
9184	BUB3	1	0.03	0.95	16/99	1	
6597	SMARCA4	4	0.05	0.94	49/99	2	
6605	SMARCE1	1	0.03	0.94	26/99	1	
6429	SRSF4	1	0.05	0.93	27/99	2	
25873	RPL36	3	0.03	0.93	76/99	2	
5955	RCN2	1	0.03	0.93	18/99	1	
54888	NSUN2	1	0.02	0.93	30/99	1	
5162	PDHB	1	0.02	0.93	30/99	1	
51649	MRPS23	1	0.04	0.92	33/99	2	
6626	SNRPA	4	0.04	0.92	72/99	2	
1072	CFL1	1	0.03	0.92	21/99	1	
7431	VIM	8	0.06	0.90	72/99	2	
2617	GARS	1	0.03	0.90	24/99	1	
6122	RPL3	9	0.04	0.89	95/99	2	
26354	GNL3	1	0.03	0.89	23/99	1	
6194	RPS6	4	0.03	0.88	80/99	2	
170506	DHX36	2	0.04	0.87	50/99	2	
509	ATP5C1	1	0.03	0.87	24/99	1	
9188	DDX21	13	0.06	0.86	87/99	2	
808	CALM3	1	0.06	0.86	7/99	1	
117246	FTSJ3	2	0.04	0.85	43/99	2	
8607	RUVBL1	3	0.05	0.84	51/99	2	
821	CANX	1	0.03	0.84	16/99	1	
55922	NKRF	2	0.03	0.84	57/99	2	
10946	SF3A3	2	0.35	0.83	11/99	2	
55226	NAT10	1	0.03	0.82	20/99	1	
79084	WDR77	1	0.03	0.82	28/99	1	
5501	PPP1CC	1	0.02	0.82	36/99	1	
10607	TBL3	1	0.25	0.81	8/99	2	
1460	CSNK2B	1	0.07	0.80	5/99	1	
26073	POLDIP2	1	0.05	0.80	25/99	2	
1656	DDX6	3	0.04	0.79	48/99	1	
51631	LUC7L2	2	0.04	0.79	49/99	2	

11224	RPL35	2	0.03	0.79	69/99	2	
10146	G3BP1	4	0.16	0.78	40/99	2	
3304	HSPA1B	76	0.12	0.78	99/99	2	inducible HSP70
11051	NUDT21	2	0.04	0.78	49/99	2	
79039	DDX54	1	0.03	0.77	18/99	1	
83858	ATAD3B	2	0.13	0.75	18/99	2	
6124	RPL4	7	0.04	0.75	98/99	2	
178	AGL	5	0.09	0.73	54/99	2	
6633	SNRPD2	5	0.04	0.73	85/99	2	
2194	FASN	9	0.07	0.72	71/99	2	
10291	SF3A1	3	0.76	0.71	6/99	2	
11052	CPSF6	2	0.04	0.68	52/99	2	
6210	RPS15A	4	0.03	0.68	89/99	2	
191	AHCY	4	0.10	0.67	58/99	2	
51081	MRPS7	1	0.03	0.67	16/99	1	
6636	SNRPF	1	0.03	0.67	44/99	2	
3305	HSPA1L	39	0.09	0.66	98/99	2	
10856	RUVBL2	4	0.04	0.65	64/99	2	
55210	ATAD3A	2	0.11	0.63	17/99	2	
3008	HIST1H1E	5	0.03	0.63	93/99	2	
8106	PABPN1	1	0.02	0.63	51/99	1	
23223	RRP12	1	0.06	0.62	24/99	2	
23112	TNRC6B	11	0.05	0.62	86/99	2	
22894	DIS3	1	0.05	0.62	12/99	1	
4176	MCM7	2	0.04	0.62	43/99	2	
51593	SRRT	1	0.02	0.61	53/99	1	
26057	ANKRD17	1	0.63	0.60	3/99	2	
8531	CSDA	6	0.05	0.60	66/99	2	
55037	PTCD3	1	0.03	0.60	24/99	1	
56257	MEPCE	1	0.05	0.59	9/99	1	
3313	HSPA9	25	0.07	0.55	99/99	2	
23450	SF3B3	3	0.03	0.55	70/99	2	
6428	SRSF3	3	0.03	0.51	84/99	2	
10528	NOP56	1	0.03	0.51	25/99	1	
1665	DHX15	7	0.04	0.50	94/99	2	
23636	NUP62	1	0.23	0.49	8/99	2	
6627	SNRPA1	2	0.03	0.49	63/99	2	
11137	PWP1	1	0.02	0.48	33/99	1	
8087	FXR1	1	0.03	0.47	29/99	1	
56945	MRPS22	2	0.04	0.46	47/99	2	
6181	RPLP2	9	0.04	0.46	99/99	2	
6146	RPL22	2	0.02	0.46	88/99	1	
1736	DKC1	1	0.04	0.44	17/99	1	
7284	TUFM	3	0.03	0.43	69/99	2	
6949	TCOF1	1	0.07	0.42	6/99	1	
60	ACTB	6	0.04	0.42	86/99	2	
25940	FAM98A	2	0.03	0.42	62/99	2	
55131	RBM28	1	0.02	0.40	32/99	1	
6168	RPL37A	1	0.02	0.40	47/99	1	
8899	PRPF4B	1	0.06	0.39	7/99	1	

8471	IRS4	4	0.06	0.37	51/99	2
8971	H1FX	1	0.02	0.37	42/99	1
8480	RAE1	1	0.04	0.36	15/99	1
9045	RPL14	3	0.02	0.36	95/99	2
6137	RPL13	4	0.03	0.35	87/99	2
6191	RPS4X	6	0.03	0.34	95/99	2
10492	SYNCRIP	6	0.04	0.33	85/99	2
6431	SRSF6	1	0.02	0.33	46/99	1
3191	HNRNPL	4	0.03	0.32	86/99	2
1933	EEF1B2	1	0.02	0.32	60/99	2
23107	MRPS27	1	0.02	0.31	45/99	1
10427	SEC24B	2	0.11	0.30	39/99	2
3192	HNRNPU	15	0.05	0.29	98/99	2
5315	PKM2	5	0.05	0.29	72/99	2
3895	KTN1	1	0.10	0.28	3/99	1
8833	GMPS	1	0.05	0.26	10/99	1
6202	RPS8	4	0.03	0.26	91/99	2
6628	SNRPB	5	0.03	0.26	95/99	2
2885	GRB2	1	0.08	0.25	21/99	2
1994	ELAVL1	3	0.03	0.25	84/99	2
6629	SNRPB2	1	0.02	0.25	56/99	1
9343	EFTUD2	3	0.18	0.24	32/99	2
10419	PRMT5	1	0.02	0.23	31/99	1
86	ACTL6A	1	0.02	0.23	40/99	1
391634	HSP90AB2	2	0.05	0.21	37/99	2
2197	FAU	1	0.02	0.20	55/99	1
7001	PRDX2	2	0.03	0.19	61/99	2
6147	RPL23A	3	0.03	0.19	90/99	2
6742	SSBP1	1	0.02	0.19	51/99	1
10514	MYBBP1A	3	0.07	0.18	34/99	2
3329	HSPD1	8	0.07	0.18	74/99	2
1459	CSNK2A2	1	0.07	0.18	6/99	1
3609	ILF3	8	0.04	0.18	90/99	2
9530	BAG4	4	0.03	0.18	88/99	2
6223	RPS19	4	0.03	0.18	79/99	2
6156	RPL30	2	0.03	0.18	75/99	2
6232	RPS27	1	0.02	0.18	51/99	1
6136	RPL12	3	0.03	0.17	91/99	2
9092	SART1	1	0.06	0.16	8/99	1
6222	RPS18	5	0.03	0.16	90/99	2
6193	RPS5	1	0.02	0.15	46/99	1
10236	HNRNPR	5	0.04	0.14	84/99	2
6161	RPL32	1	0.02	0.14	56/99	2
5516	PPP2CB	1	0.02	0.14	47/99	1
220988	HNRNPA3	6	0.03	0.13	94/99	2
10016	PDCD6	1	0.02	0.13	48/99	1
10498	CARM1	1	0.03	0.12	46/99	2
9349	RPL23	3	0.03	0.12	86/99	2
6135	RPL11	2	0.02	0.11	97/99	2
6601	SMARCC2	1	0.02	0.11	38/99	1

2316	FLNA	4	0.30	0.10	19/99	2	filamin
24148	PRPF6	1	0.06	0.10	7/99	1	
8452	CUL3	1	0.05	0.09	40/99	2	
6160	RPL31	2	0.02	0.08	92/99	2	
26227	PHGDH	1	0.02	0.08	45/99	1	
1973	EIF4A1	2	0.04	0.06	44/99	1	
7818	DAP3	1	0.03	0.05	52/99	2	
10189	THOC4	2	0.02	0.05	77/99	1	
871	SERPINH1	1	0.02	0.05	45/99	1	
1778	DYNC1H1	1	0.09	0.04	25/99	2	
27335	EIF3K	1	0.07	0.04	4/99	1	
3326	HSP90AB1	7	0.04	0.04	86/99	2	
9782	MATR3	2	0.03	0.03	61/99	2	
10432	RBM14	3	0.03	0.02	77/99	2	
6207	RPS13	3	0.03	0.02	83/99	2	
51386	EIF3L	3	0.09	0.01	16/99	1	
10131	TRAP1	1	0.02	0.01	77/99	1	
6631	SNRPC	2	0.02	0.01	93/99	2	
6430	SRSF5	1	0.03	0.00	50/99	2	
6741	SSB	1	0.01	-1.13	94/99	2	
203068	TUBB	10	0.04	-1.12	99/99	2	
51493	C22orf28	1	0.01	-1.09	95/99	2	
3858	KRT10	4	0.03	-1.05	98/99	2	
10383	TUBB2C	9	0.04	-0.95	91/99	2	
1654	DDX3X	11	0.04	-0.93	99/99	2	
6635	SNRPE	1	0.01	-0.92	91/99	2	
6141	RPL18	2	0.02	-0.90	97/99	2	
3181	HNRNPA2E	8	0.04	-0.82	99/99	2	
3190	HNRNPK	7	0.04	-0.80	99/99	2	
54431	DNAJC10	2	0.02	-0.80	93/99	2	
4691	NCL	14	0.05	-0.78	97/99	2	
3185	HNRNPF	5	0.03	-0.72	98/99	2	
3188	HNRNPH2	5	0.03	-0.72	88/99	2	
6138	RPL15	2	0.02	-0.68	94/99	2	
26986	PABPC1	10	0.04	-0.67	98/99	2	
7073	TIAL1	3	0.03	-0.67	92/99	2	
3848	KRT1	19	0.06	-0.66	99/99	2	
2521	FUS	13	0.05	-0.65	99/99	2	
1660	DHX9	13	0.05	-0.64	98/99	2	
6188	RPS3	6	0.03	-0.64	99/99	2	
3921	RPSA	4	0.03	-0.64	98/99	2	
3849	KRT2	8	0.04	-0.63	95/99	2	
3178	HNRNPA1	7	0.04	-0.60	99/99	2	
1653	DDX1	3	0.02	-0.60	98/99	2	
6234	RPS28	2	0.02	-0.58	96/99	2	
292	SLC25A5	1	0.02	-0.58	78/99	1	
7295	TXN	1	0.02	-0.55	83/99	2	
23367	LARP1	1	0.02	-0.55	76/99	1	
6203	RPS9	1	0.02	-0.54	80/99	1	
9131	AIFM1	1	0.02	-0.51	68/99	2	

6128	RPL6	5	0.03	-0.50	96/99	2
1655	DDX5	7	0.04	-0.49	96/99	2
6175	RPLP0	5	0.03	-0.49	98/99	2
3301	DNAJA1	1	0.02	-0.48	69/99	2
293	SLC25A6	1	0.02	-0.46	57/99	1
3608	ILF2	3	0.02	-0.45	95/99	2
6129	RPL7	3	0.03	-0.44	90/99	2
10949	HNRNPA0	1	0.02	-0.44	79/99	1
3308	HSPA4	3	0.03	-0.43	78/99	2
3861	KRT14	2	0.04	-0.42	72/99	2
6125	RPL5	5	0.03	-0.42	96/99	2
3189	HNRNPH3	5	0.03	-0.40	99/99	2
8761	PABPC4	7	0.04	-0.39	86/99	2
6134	RPL10	2	0.02	-0.39	90/99	1
3184	HNRNPD	4	0.03	-0.38	98/99	2
51637	C14orf166	2	0.02	-0.38	87/99	2
10575	CCT4	1	0.02	-0.38	72/99	1
6389	SDHA	1	0.01	-0.38	81/99	1
3852	KRT5	3	0.04	-0.37	67/99	2
10642	IGF2BP1	3	0.03	-0.37	85/99	2
6230	RPS25	2	0.02	-0.37	87/99	2
83743	GRWD1	1	0.02	-0.36	77/99	2
6950	TCP1	1	0.02	-0.36	59/99	1
10342	TFG	30	0.07	-0.35	99/99	2
6632	SNRPD1	6	0.03	-0.35	96/99	2
6169	RPL38	1	0.02	-0.35	74/99	1
6159	RPL29	1	0.01	-0.33	90/99	2
3187	HNRNPH1	12	0.05	-0.32	98/99	2
6204	RPS10	2	0.02	-0.32	87/99	2
6209	RPS15	2	0.02	-0.32	81/99	2
7314	UBB	2	0.03	-0.31	93/99	2
908	CCT6A	1	0.02	-0.31	55/99	1
11100	HNRNPUL1	17	0.06	-0.30	99/99	2
708	C1QBP	4	0.03	-0.30	95/99	2
10808	HSPH1	2	0.03	-0.30	68/99	2
4343	MOV10	1	0.02	-0.30	64/99	1
1915	EEF1A1	6	0.05	-0.29	98/99	2
7203	CCT3	1	0.02	-0.29	50/99	1
26156	RSL1D1	1	0.02	-0.28	60/99	2
6231	RPS26	1	0.02	-0.28	73/99	1
9987	HNRPDL	3	0.03	-0.27	89/99	2
6130	RPL7A	5	0.03	-0.27	96/99	2
5725	PTBP1	1	0.02	-0.27	60/99	1
2597	GAPDH	1	0.02	-0.27	73/99	2
6432	SRSF7	1	0.02	-0.27	54/99	2
10576	CCT2	2	0.06	-0.26	65/99	2
10574	CCT7	1	0.05	-0.26	46/99	2
5351	PLOD1	3	0.03	-0.26	87/99	2
498	ATP5A1	2	0.03	-0.25	75/99	2
6139	RPL17	2	0.02	-0.25	78/99	2

6228	RPS23	1	0.02	-0.25	78/99	1
6144	RPL21	3	0.03	-0.24	92/99	2
8335	HIST1H2AE	1	0.02	-0.23	65/99	2
3182	HNRNPAB	4	0.03	-0.22	99/99	2
7531	YWHAE	1	0.03	-0.21	56/99	1
6224	RPS20	3	0.02	-0.21	94/99	2
10521	DDX17	9	0.04	-0.20	96/99	2
6187	RPS2	5	0.03	-0.20	93/99	2
1832	DSP	1	0.03	-0.20	42/99	1
10130	PDIA6	1	0.02	-0.20	66/99	1
6155	RPL27	2	0.02	-0.20	84/99	2
790	CAD	9	0.05	-0.18	87/99	2
4869	NPM1	6	0.03	-0.18	96/99	2
4522	MTHFD1	1	0.02	-0.18	53/99	1
6229	RPS24	3	0.02	-0.18	96/99	2
6142	RPL18A	1	0.02	-0.18	62/99	1
5591	PRKDC	1	0.02	-0.18	42/99	1
27161	EIF2C2	2	0.02	-0.17	67/99	1
11338	U2AF2	1	0.02	-0.17	55/99	1
10376	TUBA1B	9	0.05	-0.15	75/99	2
9919	SEC16A	1	0.03	-0.15	50/99	1
3838	KPNA2	2	0.03	-0.15	79/99	1
55015	PRPF39	1	0.03	-0.15	53/99	2
9958	USP15	1	0.03	-0.15	41/99	1
5111	PCNA	1	0.02	-0.15	64/99	1
4172	MCM3	1	0.02	-0.14	46/99	1
6157	RPL27A	1	0.02	-0.14	65/99	1
1642	DDB1	1	0.02	-0.13	54/99	1
8661	EIF3A	1	0.05	-0.12	16/99	1
6201	RPS7	3	0.03	-0.12	79/99	2
6133	RPL9	3	0.03	-0.12	85/99	2
8663	EIF3C	1	0.05	-0.11	14/99	1
10971	YWHAQ	1	0.02	-0.11	45/99	1
85236	HIST1H2BK	2	0.02	-0.11	84/99	2
4673	NAP1L1	2	0.02	-0.11	84/99	2
6426	SRSF1	2	0.03	-0.10	73/99	2
23517	SKIV2L2	1	0.02	-0.10	49/99	1
3857	KRT9	14	0.06	-0.09	88/99	2
22824	HSPA4L	2	0.04	-0.09	50/99	2
5706	PSMC6	1	0.04	-0.09	34/99	1
7534	YWHAZ	1	0.03	-0.09	31/99	1
9733	SART3	3	0.11	-0.08	57/99	2
8148	TAF15	5	0.03	-0.08	92/99	2
3183	HNRNPC	4	0.03	-0.08	88/99	2
22907	DHX30	3	0.03	-0.08	70/99	2
476	ATP1A1	1	0.02	-0.08	39/99	1
8668	EIF3I	1	0.05	-0.07	18/99	1
2130	EWSR1	6	0.03	-0.07	97/99	2
4736	RPL10A	3	0.03	-0.07	81/99	2
192111	PGAM5	1	0.04	-0.06	17/99	1

8239	USP9X	1	0.04	-0.06	21/99	1
1938	EEF2	5	0.03	-0.06	91/99	2
6637	SNRPG	2	0.02	-0.06	85/99	2
8662	EIF3B	2	0.32	-0.05	14/99	2
3054	HCFC1	2	0.54	-0.04	11/99	2
8667	EIF3H	1	0.08	-0.04	7/99	1
8664	EIF3D	1	0.06	-0.04	14/99	1
9128	PRPF4	1	0.05	-0.04	17/99	1
6218	RPS17	2	0.03	-0.03	75/99	2
4076	CAPRIN1	2	0.10	-0.02	54/99	2
3309	HSPA5	27	0.07	-0.02	99/99	2
8454	CUL1	1	0.07	-0.02	6/99	1
6217	RPS16	5	0.03	-0.02	98/99	2
1981	EIF4G1	1	0.37	-0.01	7/99	2
10594	PRPF8	3	0.19	-0.01	45/99	2
23020	SNRNP200	3	0.18	-0.01	46/99	2
6500	SKP1	1	0.04	-0.01	26/99	1
7532	YWHAG	1	0.03	-0.01	25/99	1
4686	NCBP1	1	0.02	-0.01	55/99	1